Pseudotyped lentiviral vectors for gene therapy: impact of envelope glycoproteins

Rodrigo José Gameiro Nogueira

Dissertation to obtain a

Master's degree in Medical Microbiology

October 2019

Pseudotyped lentiviral vectors for gene therapy: impact of envelope glycoproteins

Rodrigo José Gameiro Nogueira

Dissertation to obtain a

Master's degree in Medical Microbiology

Supervisors:
Doctor Ana Sofia Coroadinha, iBET & ITQB - NOVA
Doctor Ana Filipa Rodrigues, iBET & ITQB - NOVA
Prof. Doctor João Piedade, IHMT - NOVA

Instituto de Tecnologia Química e Biológica António Xavier (ITQB - NOVA)
Instituto de Biologia Experimental e Tecnológica (iBET)
Universidade NOVA de Lisboa
(Cell Line Development and Molecular Biotechnology Laboratory, Animal Cell Technology Unit)

October 2019

Acknowledgements

I would like to express my gratitude to everyone who, directly or indirectly, contributed to this work.

To my supervisor Dr. Ana Sofia Coroadinha, for giving me the opportunity to develop this thesis in the Cell Line Development and Molecular Biotechnology Laboratory, for the supervision and scientific guidance.

A special acknowledgment to my supervisor Dr. Ana Filipa Rodrigues, for the constant support, scientific and technical guidance, advices and the encouragement that kept me going, even when all seemed difficult. Thank you for all the patience and the help throughout this entire journey. I am sure that this year would have been a lot more difficult without your guidance.

To my friends and colleagues from the CLD&MB: Ana Isabel, Ana Oliveira, Sofia, Miguel and Hélio for help, the advices and for making me feel a part of the team. A special acknowledgment to Maria, Elisa, Catarina, Mariana and Tiago for always being there for me, for the good times, the constant support and for making me laugh, even in the most challenging days.

Aos meus pais e à minha irmã. Obrigado por terem feito o que era possível e o que era impossível para que eu pudesse estar onde estou hoje. Obrigado por todo o apoio, pela compreensão, pelo exemplo de perseverança e por terem acreditado em mim, mesmo quando eu não era capaz. Esta tese é dedicada a vocês.

Abstract

The potential of gene therapy to treat a broad range of diseases, ranging from cancer to monogenic diseases, makes it a powerful approach to address medical needs that are currently unmet by conventional medicine. Lentiviral vectors have been the viral vectors experiencing the highest growth in gene therapy clinical trials due to their large genetic payload, the ability to transduce both dividing and non-dividing cells, permanently integrating into the target cell genome and increased safety when compared to *Gammaretrovirus.* However, the utilization of lentiviral vectors in gene therapy has been conditioned by the currently available production systems. The development of constitutive producer cell lines will provide a better alternative to cope with the increasing necessity of large-scale production of lentiviral vectors.

This work focused on the evaluation of GaLV10A1$^{\Delta R}$ envelope glycoprotein potential for stable expression, in order to enable its use in constitutive producer cells. This was based on a previously developed cell line, HEK 293T SLC20A1 knock-out, especially designed to cope with the cytotoxicity of GaLV10A1$^{\Delta R}$. To achieve stable expression of GaLV envelope glycoproteins new plasmids were constructed. An analytical method for syncytia quantification, based on cell size distribution, was also successfully developed. This work showed that SLC20A1 deletion enabled GaLV10A1$^{\Delta R}$ expression, eliminating the cytotoxicity associated with its expression. More importantly, SLC20A1 knock-out enabled the establishment of a cell population stably expressing GaLV10A1$^{\Delta R}$. SLC20A1 deletion led to a decrease in cell growth, however it was restored by SLC20A2 complementation. Altogether, this thesis supports the viral receptor knock-out strategy to develop new cell lines to express glycoproteins with fusogenicity-derived cytotoxicity and provides new insights that will help improve this strategy.

This work contributes to the state-of-the-art of the lentiviral vector-based gene therapy, providing new insights that will improve the development of constitutive producer cells in the near future.

Resumo

O potencial da terapia génica para tratar um largo espetro de doenças, desde o cancro até monogénicas, torna-a uma abordagem poderosa para colmatar necessidades médicas que atualmente não são atendidas pela medicina convencional. Os vetores lentivirais foram os vetores virais que apresentaram o maior crescimento em ensaios clínicos de terapia génica. Isto deve-se à sua grande carga genética, à capacidade de transduzir células em divisão e não-divisão, integração permanente no genoma da célula hospedeira e maior segurança comparativamente aos *Gammaretrovirus.* No entanto, a sua utilização em terapia génica é condicionada pelos sistemas de produção de vetores lentivirais atualmente disponíveis. O desenvolvimento de linhas celulares produtoras constitutivas será uma melhor alternativa para lidar com a necessidade crescente de sistema de produção em larga escala de vetores lentivirais.

Este trabalho avaliou a potencial utilização da glicoproteína GaLV10A1$^{\Delta R}$ em expressão estável, com o objetivo de permitir a sua utilização no estabelecimento de linhas celulares produtoras constitutivas. Este trabalho baseou-se numa linha celular já desenvolvida, HEK 293T SLC20A1 KO, especialmente projetada para lidar com a citotoxicidade de GaLV10A1$^{\Delta R}$. Aqui, construímos novos plasmídeos capazes de expressar glicoproteínas estavelmente. Desenvolvemos também um método analítico de quantificação de sincícios. Este trabalho mostrou que é possível eliminar a citotoxicidade associada com GaLV10A1$^{\Delta R}$ através da deleção de SLC20A1. Mostrámos também que a deleção de SLC20A1 permitiu a expressão estável de GaLV10A1$^{\Delta R}$. A deleção desta proteína levou à diminuição do crescimento HEK 293T SLC20A1 KO, no entanto, este foi recuperado com a sobreexpressão de SLC20A2. Em conclusão, este trabalho suporta a estratégia baseada na deleção de recetores virais para a expressão estável de glicoproteinas citotóxicas.

Esta tese contribui para o estado da arte da terapia génica baseada em vetores lentivirais, fornecendo novo conhecimento que permitirá melhorar o desenvolvimento de linhas celulares produtoras constitutivas num futuro próximo.

Keywords

Gene therapy; Lentiviral vectors; Envelope glycoproteins; Stable expression; Constitutive producer cell lines.

Palavras-chave

Terapia génica; Vetores lentivirais; Glicoproteínas do invólucro; Expressão estável; Linhas celulares produtoras constitutivas

List of Contents

Figure Index

Table Index

Abbreviations

AIDS	Acquired immunodeficiency syndrome
ALB	Albumin
CA	Capsid protein
CMV	Cytomegalovirus
cPPT	Central polypurine tract
Ct	Cycle threshold
DMEM	Dulbecco's modified Eagle's medium
eGFP	Enhanced green fluorescence protein
EMCV	Encephalomyocarditis virus
Env	Envelope glycoprotein
FBS	Fetal bovine serum
ferH	Ferritin heavy chain
FIV	Feline immunodeficiency virus
FMDV	Foot-and-mouth disease virus
GaLV	Gibbon ape leukemia virus
HBB2	Hemoglobin subunit beta-2
HEK	Human embryonic kidney
HIV-1	Human immunodeficiency virus type 1
HIV-2	Human immunodeficiency virus type 2
hPGK	Human phosphoglycerate kinase 1
$Hygro^R$	Hygromycin resistance marker
I.P.	Infectious particles
IN	Integrase
IRES	Internal ribosome entry site
KO	Knock-out
LTR	Long terminal repeats
LV	Lentiviral vector
MA	Matrix protein
mEF1α	Mouse elongation factor 1 alpha
MLV	Murine leukemia virus
MOI	Multiplicity of infection
NC	Nucleocapsid protein
PBS	Phosphate-buffered saline
PEI	Polyethylenimine

PiT-1	Phosphate transporter 1 (alternative name for Sodium-dependent phosphate transporter 1)
PiT-2	Phosphate transporter 2 (alternative name for Sodium-dependent phosphate transporter 2)
PPT	Polypurine tract
PR	Protease
RBG	Rabbit beta-globin intron
RCL	Replication-competent lentiviruses
Rev	Regulator of expression of viral proteins
RRE	Rev responsive element
RSV	Rous sarcoma virus
RT	Reverse transcriptase
RT-qPCR	Real-time quantitative PCR
SIN	Self-inactivating
SIV	Simian immunodeficiency virus
sgRNA	Single guide RNA
SLC20A1	Sodium-dependent phosphate transporter 1
SLC20A2	Sodium-dependent phosphate transporter 2
SU	Surface domain of envelope glycoprotein
SV40	Simian virus 40
T.U.	Transducing units
TAR	Tat responsive element
Tat	Trans-activator of transcription
TBS	Tris-buffered saline
TF	Trans-frame protein
TM	Transmembrane domain of envelope glycoprotein
U3	3’ untranslated region
U5	5’ untranslated region
VCN	Vector copies *per* nucleus
VSV-G	Vesicular stomatitis virus G glycoprotein

1. Introduction

1.1. Therapeutic potential of viral vectors for gene therapy

Gene therapy is defined as the transfer of genetic material into a patients' cells to treat or prevent diseases. It is considered a revolutionary medical approach and has been used to treat cancer, monogenic, infectious or cardiovascular diseases (**Figure 1.1 A**) [1–3].

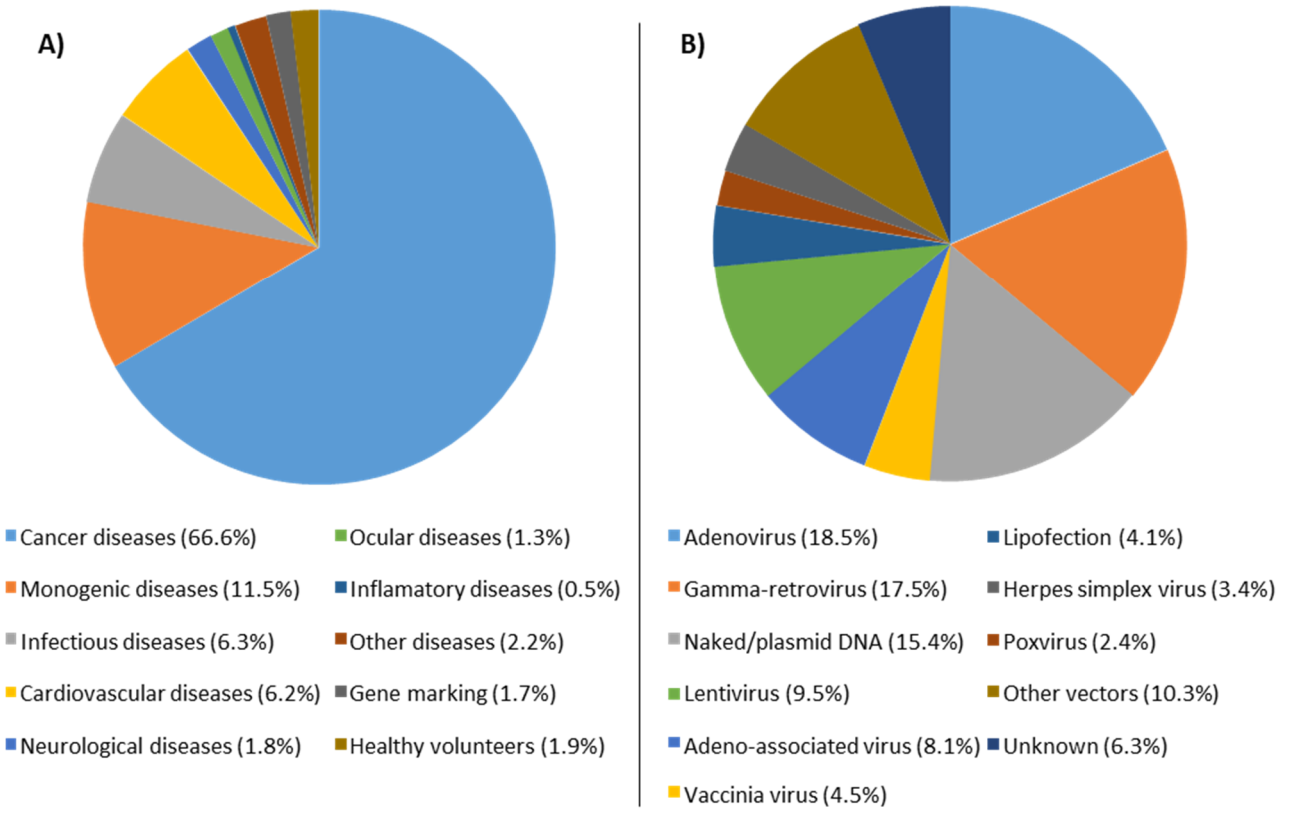

Figure 1. 1 – Gene therapy clinical trials worldwide. A) Diseases targeted and B) delivery vectors used in gene therapy clinical trials (Source: Gene Therapy Clinical Trials Worldwide database [2], accessed: September 13th 2019).

Since 1989, when the first gene therapy clinical trial was performed using transduced cells with retroviral vectors to treat patients with advanced melanoma [4], more than 2900 trials have been conducted or are still ongoing [2]. Also, several gene therapy products have received market approval.

In 2018, the market size for gene therapy was valued at USD 536.43 million dollars with prospects to keep growing [5]. By 2026, gene therapy market value is estimated to be worth USD 5.55 billion dollars, due to the increasing incidence of cancer and chronic diseases and the targeting of some rare diseases that are untreatable by conventional medical approaches [6].

Depending on the disease and target cells or tissues to be treated, gene therapy can be performed *in vivo* or *ex vivo*. In the former strategy, the genetic material is directly administered into the patient. In the latter, the target cells are harvested, genetically modified and re-administered into the patient [3,7]. The introduction of the therapeutic transgene into the target cells is mediated by delivery vehicles that can be

divided into non-viral and viral vectors [3,8]. Viral vectors are currently the most used vectors in gene therapy clinical trials, comprising nearly 70% of all delivery vectors (**Figure 1.1 B**) [2]. Among the several viruses, the most used viral vectors in gene therapy are derived from *Gammaretrovirus*, *Lentivirus*, *Adenovirus* and *Adeno-associated virus* [2].

Lentiviral vectors (LV) are currently the gene therapy vector experiencing the highest growth of usage in clinical trials (**Figure 1.2**) [2]. These vectors are characterized by: i) the ability to permanently integrate into the target cell genome allowing life-long expression of the transgene in transduced cells and their progeny; ii) transduce both dividing and non-dividing cells; ii) a large genetic payload capacity (up to 9 kb); iv) a lower risk of insertional mutagenesis when compared to their simpler counterparts *Gammaretrovirus* and v) minimal immune response when used *in vivo*; [9–12]. This set of characteristics makes them the vector of choice for applications that require long-term expression of the transgene.

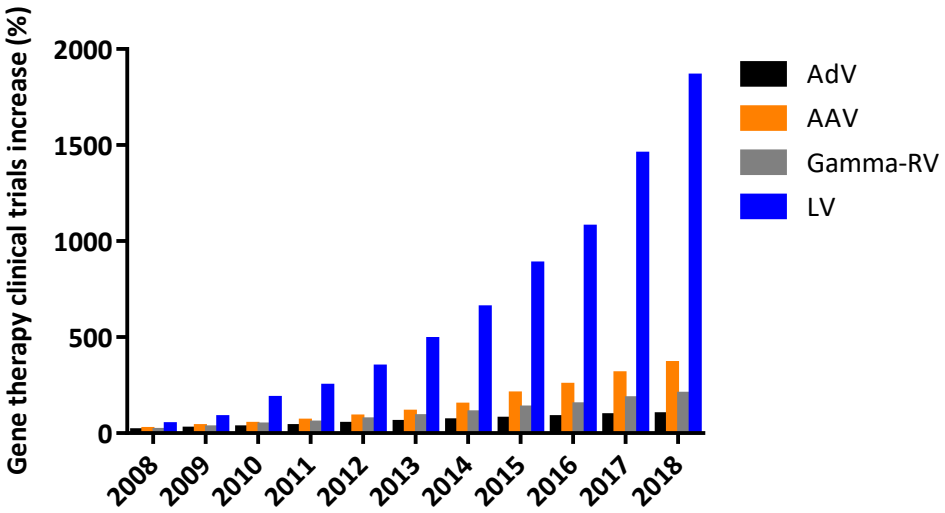

Figure 1. 2 – Gene clinical trials increase between 2008 and 2018. Increase, in percentage (%), of utilization of different viral vectors in gene therapy clinical trials, comparatively to 2007. *Adenovirus* (AdV), *Adeno-associated virus* (AAV), *Gammaretrovirus* (Gamma-RV) and *Lentivirus* (LV). (Source: Gene Therapy Clinical Trials Worldwide database [2], accessed: September 13th 2019).

In 2017, the first cell therapy product using LV based gene therapy, named KYMRIAH (Novartis), was approved by the U.S. Food and Dugs Administration. KYMRIAH uses LV to modify autologous T lymphocytes, into CAR-T cells, to treat B-cell acute lymphoblastic leukemia and large B-cell lymphoma [13].

1.2. Lentiviruses biology

Lentiviruses are classified as one of the eleven genera comprising the *Retroviridae* family [14]. This genus is composed by ten human and non-human pathogens, such as the human immunodeficiency virus type 1 and type 2 (HIV-1/ HIV-2), the simian immunodeficiency virus (SIV) and feline immunodeficiency virus (FIV) [14]. Lentiviruses are characterized by causing chronic infections usually associated to long incubation periods [15,16]. Among *Lentivirus*, HIV-1 became one of the most studied and understood virus, due to its

highly pathogenic nature that may generate the acquired immunodeficiency syndrome (AIDS) [17,18] with major social and economic impact [19].

HIV-1 (**Figure 1.3**) is an enveloped virus composed of two copies of linear positive-sense, single-strand RNA. It is characterized by a unique replicative strategy, transversal to all retroviruses, where the viral RNA genome is reverse transcribed into double strand DNA – proviral DNA – prior to stable integration into the host cell genome [20–22]. HIV-1 are spherical viruses with approximately 80-120 nm in diameter [23]. Its cone-shape capsid is composed by the capsid (CA) protein and contains the viral genome surrounded by the nucleocapsid (NC) protein, as well as the reverse transcriptase (RT), integrase (IN), protease (PR) and the accessory proteins. This viral capsid is enclosed inside another protein shell formed by the matrix (MA) protein which is surrounded by a lipid bilayer derived from the host cellular membrane. Anchored in this lipid bilayer is the envelope glycoprotein (Env), constituted by two protein subunits, the transmembrane (TM) and the surface (SU) domain. The envelope glycoproteins are responsible for cell surface receptor recognition and mediate the entry into the host cell [22,24].

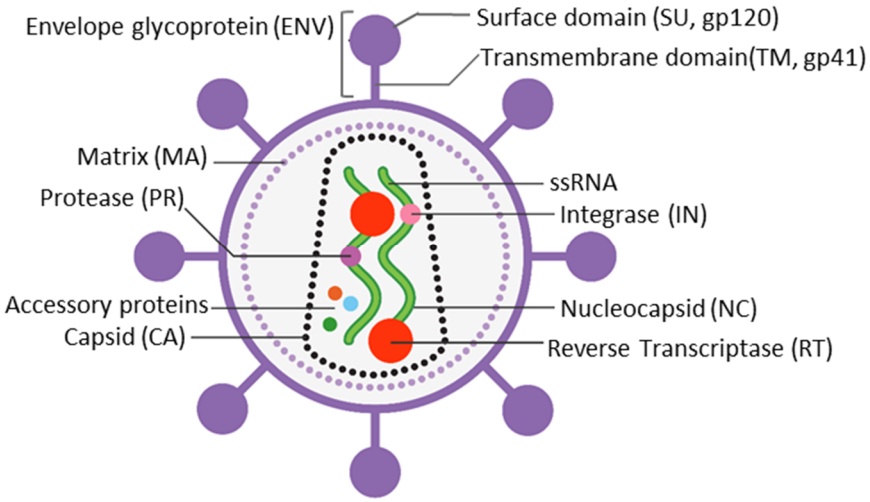

Figure 1. 3 – Schematic representation of the HIV-1 particle structure. Adapted from [25] (accessed: 23rd September 2019).

The HIV-1 genome (**Figure 1.4**) is composed of several non-coding sequences that control gene expression and protein synthesis and three genes encoding the enzymatic and structural proteins, transversal to all retrovirus. Additionally, it contains six genes encoding accessory and regulatory proteins, unique to lentivirus [22].

The *gag* gene encodes the Gag polyprotein. This polyprotein is proteolytically processed by the PR, to originate the three main structural proteins (MA, CA and NC) as well as the trans-frame (TF) protein. The *gag* and *pol* genes encode the Gag-Pro-Pol polyprotein after a ribosomal frameshift. This polyprotein encodes the main structural proteins as well as the RT, PR and IN. The last three enzymes are responsible for reverse transcription of the viral RNA, maturation of the virion and integration of the proviral DNA into the host

genome, respectively. The *env* gene encodes the Env polyprotein that originates the TM and SU subunits after proteolytic processing by cellular proteases [23,24,26].

The *tat* and *rev* genes encode the regulatory proteins trans-activator of transcription (Tat) and regulator of expression of viral proteins (Rev). These increase the transcription efficiency of the proviral genome and allow the nuclear export of unspliced or singly spliced mRNAs, respectively [24,27,28]. Additionally, the *vif*, *vpr*, *vpu* and *nef* genes encode accessory proteins essential for *in vivo* viral replication and pathogenesis. These proteins, however, are not necessary for *in vitro* viral replication [22,26].

Apart from these *trans*-acting sequences, HIV-1 genome is constituted by several non-coding *cis*-acting sequences. The long terminal repeats (LTR), present in the proviral genome, are constituted by a 3' untranslated region (U3), repeat elements (R) and a 5' untranslated region (U5). It contains the enhancer/promoter regulatory region as well as sequences necessary for reverse transcription and integration of the provirus into the host genome. The packaging signal (Ψ) is essential for specific packaging of full-length viral RNAs during virion assembly. The Tat responsive element (TAR) and the Rev responsive element (RRE) interact with the Tat and Rev proteins, respectively. The polypurine tract/central polypurine tract (PPT and cPPT) allow the synthesis of the positive sense DNA strand during reverse transcription. [22,23,29].

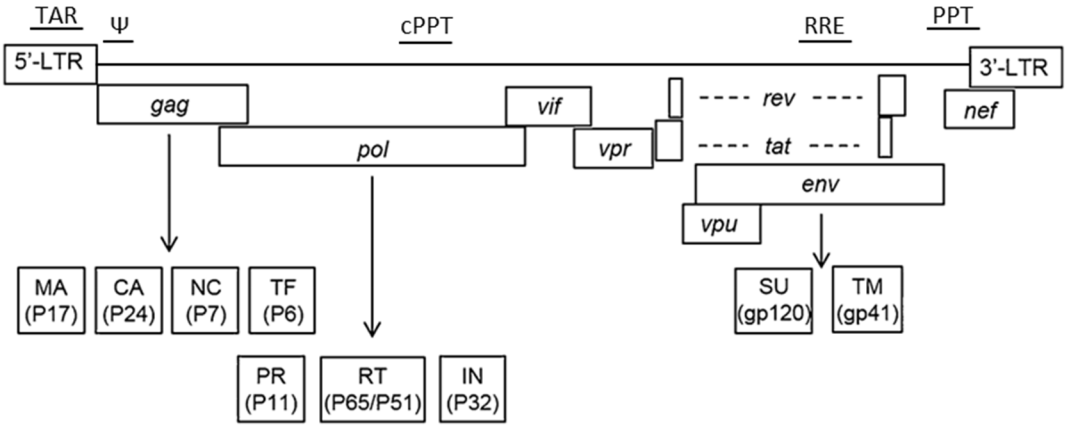

Figure 1. 4 – Schematic representation of HIV-1 proviral genome. CA: capsid protein; cPPT: central polypurine tract; IN: integrase; LTR: long terminal repeats; MA: matrix protein; NC: nucleocapsid protein; PPT: polypurine tract; RRE: Rev responsive element; Ψ: packaging signal; PPT: polypurine tract; PR: protease; RT: reverse transcriptase; SU: surface subunit; TAR: Tat responsive element; TM: transmembrane subunit; TF: trans-frame protein. Adapted from:[26].

1.3. Lentiviral vector design

To develop a LV production system, the HIV-1 genome was split into several constructs, deleting all the non-essential sequences [30]. To address biosafety concerns, specifically the formation of replication-competent lentiviruses (RCL) during LV production [31,32], four generations of LV packaging systems have been developed.

The third generation packaging system (**Figure 1.5**) developed by Dull et al. [33] is currently the most used LV production system [22,34]. It is characterized by splitting the HIV-1 genome into four independent constructs: two packaging plasmids, the envelope plasmid and the transfer plasmid [33]. The packaging plasmids encodes the structural and enzymatic genes as well as *rev*, the only HIV-1 regulatory gene retained in the third-generation system. The envelope plasmid encodes the envelope glycoprotein, usually the G-glycoprotein from the vesicular stomatitis virus (VSV-G). The transfer plasmid encodes the gene of interest and the *cis*-acting sequences necessary for packaging, reverse transcription and integration of the transgene cassette [33,35]. This split genome approach allowed the creation of non-overlapping plasmids which reduces the probability of formation RCL by homologous recombination [33,34]. To further increase the biosafety level of this system, a partial deletion in the U3 region from the 3'LTR (ΔU3 3'LTR) of the transfer vector was performed generating a self-inactivating (SIN) LV [36]. These vectors become transcriptionally inactive upon reverse transcription inside the transduced cell. Since the 5´LTR is no longer functional, it prevents vector mobilization upon infection with the wild-type HIV-1. It also decreases the risk of insertional mutagenesis linked to LTR promoter interference, without impairing LV productivity and transduction efficiency [32,35–37].

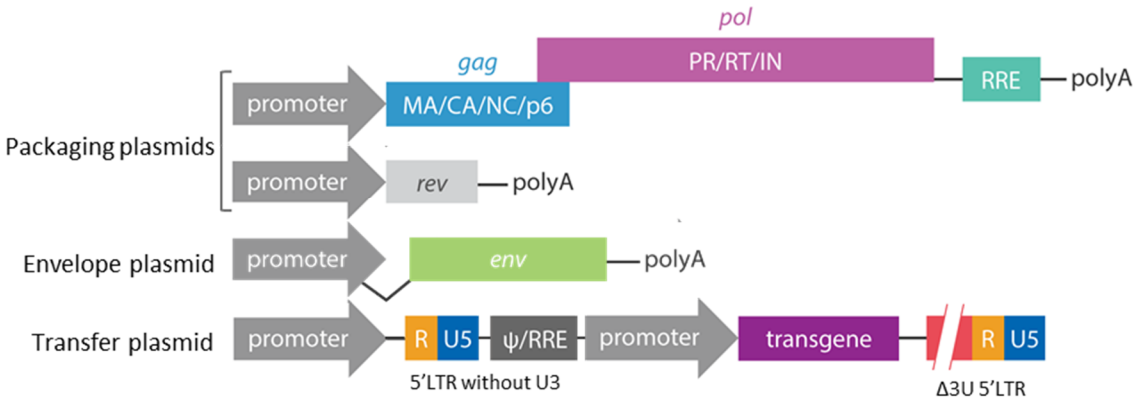

Figure 1. 5 – Schematic representation of the third generation LV packaging system. Adapted from [25] (accessed: 23rd September 2019).

A fourth generation of LV packaging systems has also been developed making this system Rev-independent [38–41]. However, the lower LV titers obtained relatively to those achieved with the second or third generation have reduced the interest this system [29].

1.4. Lentiviral vector production

LV production for research and clinical applications can be performed by transient transfection or by establishing stable producer cell lines. Most of LV production has heavily relied in the first strategy [35]. The Human Embryonic Kidney (HEK) 293 cell line and HEK 293 expressing the simian virus 40 (SV40) Large T antigen (HEK 293T) have been the most used cell substrates for LV production [22,34]. The latter are the most used due to increased cell growth, higher transfection efficiencies and superior LV titers [34,35].

For transient production, cells are co-transfected with the different plasmids of a lentiviral packaging system, and the LV containing supernatant is harvested 48 hours to 72 hours post-transfection [35]. For small-scale production, this method is fast, versatile and easy to perform, delivering titers up to 10^8 infectious particles *per* mL. However, it is difficult to scale-up and expensive, due to the need for large amounts of high-quality plasmid DNA. It is also associated with high batch-to-batch variability [22,29,34].

The increasing growth of LV usage in gene therapy clinical trials and the already consolidated transition to market requires more efficient and cost-effective methods for large-scale production [34]. This can be achieved with stable LV producer cell lines [22,42]. Stable producer cells are established by co-transfecting the cell substrate with all the component of the LV packaging system, followed by selection of the high titer clones [29,43]. Despite the time-consuming process in their development, stable producer cells represent a more cost-effective, scalable and standardized LV production platform [22,29,44].

However, the development of stable LV producer cell lines has been hindered mainly due to the cytotoxic effects associated to the expression of the viral protease and VSV-G [29,35]. Different approaches have been developed to cope with this cytotoxicity, including using non-toxic envelope glycoproteins with broad cell tropism for LV pseudotyping and expressing the cytotoxic components under the control of inducible promoters [35,44]. Stable producer cell lines can be divided into: i) constitutive producer and ii) inducible producer cell lines [34]. In the former, all the components from the packaging system are constitutively expressed. In the latter, some of the LV production components are expressed under the control of inducible promoter systems [34]. Constitutive producer cells are a preferable system since LV production in inducible producer cells is restricted to short periods of time after induction [45]. Moreover, inducible producer cells require induction agents and additional LV purification steps that make LV production more expensive [29].

Until now, five constitutive LV vector producer cell lines have been described [44]. LentiPro26 [45], recently established in our laboratory, was the last constitutive producer cell line to be developed[44]. LentiPro26 tackled the cytotoxic effects associated with LV constitutive production by substituting the VSV-G for the amphotropic murine leukemia virus (MLV) 4070A envelope glycoprotein and by using a less active and, therefore less cytotoxic, HIV-1 protease [45]. This less cytotoxic HIV-1 protease was established by changing the 26^{th} amino acid from a threonine to a serine (T26S) [46]. Despite being less active, its functionality regarding viral maturation and infectivity has not been impaired [46].

1.5. Lentiviral vector pseudotyping

LVs can incorporate envelope glycoproteins from other viruses. This process, known as pseudotyping, allows the modification of LV tropism [47,48]. Pseudotyping LV with different envelope glycoproteins or engineered envelope glycoproteins enables the creation of target-specific LVs increasing their applicability in *in vivo* gene therapy [35,49,50].

Currently, VSV-G is the most used envelope glycoprotein for LV pseudotyping [48,50,51]. This preference is the result of: i) its pantropic nature associated to an ubiquitously expressed cell receptor; ii) the ability to sustain high LV titers; iii) granting improved LV stability and iv) resistance to freeze-thaw cycles [22,48,52]. However, the lack of cell/tissue specificity associated with its broad tropism and the inactivation by the human complement present in the blood compromises its utilization in *in vivo* applications [51,53]. Additionally, VSV-G is toxic to the producer cells, when constitutively expressed [34,54].

Apart from VSV-G, envelope glycoproteins from gammaretroviruses, such as the MLV 4070A and the glycoprotein derived from the gibbon ape leukemia virus (GaLV) have been used to pseudotype LVs [55,56]. These glycoproteins can be constitutively expressed without inducing cytotoxic effects on the producer cell line, making them good options for the development of constitutive LV producer cell lines [29,57]. Similarly to VSV-G, MLV 4070A can also transduce most cells [22]. GaLV10A1 envelope glycoprotein, derived from GaLV [56], exhibits a preferential tropism for hematopoietic stem cells and differentiated hematopoietic cells making them particularly interesting in clinical gene therapy for blood and immune system related disorders [49,51,55].

1.6. Envelope glycoprotein engineering for improved lentiviral vector titers

The development of LentiPro26 [45] using a less active HIV-1 protease opened the possibility to establish new constitutive LV producer cell lines with other envelope glycoproteins, namely the clinically relevant GaLV10A1 [49,56]. GaLV10A1 is derived from GaLV envelope glycoprotein, where its cytoplasmic tail was replaced by that of MLV 4070A, to increase LV particle infectivity [55,56].

Similarly to other gammaretroviral envelope glycoproteins, GaLV10A1 is a heterodimer composed of SU subunit and a TM subunit [49]. The TM subunit is subdivided in three domains: the ectodomain, the transmembrane domain and the cytoplasmic tail [49,51]. To become functional, the cytoplasmic tail is cleaved by the retroviral protease during virion maturation, releasing a small peptide – R-peptide – and triggering the fusogenic activity of the protein [58] (**Figure 1.6 A**).

In previous work from our laboratory, three new GaLV10A1 derived envelope glycoproteins were created to pseudotype LV: GaLV10A1^{pro}, GaLV10A1^{giflet} and GaLV10A1$^{\Delta R}$ [55]. In the first and second envelope glycoproteins, the retroviral protease cleavage site from MLV 4070A cytoplasmic tail (VQAL↓VLTQ) was substituted by the HIV-1 MA/CA cleavage site sequence (SQNY↓PIVQ [59]) or by a synthetic cleavage sequence (GSGIF↓LETSL [60]), respectively [55]. This synthetic sequence has been described as the most efficiently cleaved substrate by HIV-1 protease [60]. In GaLV10A1$^{\Delta R}$, the R-peptide nucleotide sequence was deleted generating a truncated version of GaLV10A1 that does not need any further proteolytic processing to become fully active (**Figure 1. 6 B**) [55].

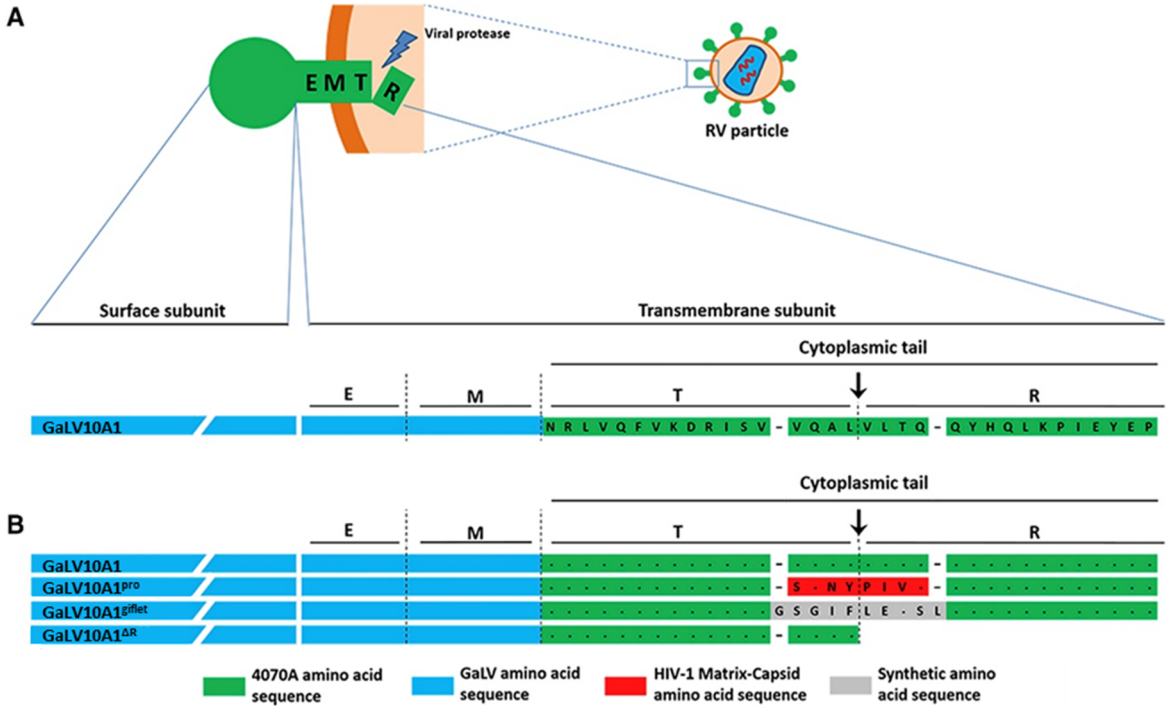

Figure 1. 6 – Schematic representation of GaLV10A1 engineered envelope glycoprotein structure. A) General structure of GaLV10A1 envelope glycoprotein. B) GaLV10A1 and GaLV10A1 engineered envelope glycoproteins (GaLV10A1^{pro} GaLV10A1^{giflet} and GaLV10A1$^{\Delta R}$) [55]. Black arrows indicate the viral protease cleavage site. E: ectodomain; M: transmembrane domain; R: R-peptide; T: cytoplasmic tail after proteolytic cleavage of the R-peptide. Adapted from [55].

With these newly developed GaLV10A1 engineered envelope glycoproteins, especially GaLV10A1$^{\Delta R}$, LV titers were substantially increased comparatively to the original GaLV10A1 envelope [55]. However, the expression of GaLV10A1$^{\Delta R}$ led to syncytia formation in the LV producer cells [55]. Despite very competitive titers, the cytotoxicity associated with its expression hindered its utilization to establish a constitutive LV producer cell line [55].

To circumvent this problem, a new HEK 293T derived cell line was developed. By using CRISPR/Cas9 genome editing system, the GaLV10A1 cell receptor was deleted from HEK 293T (unpublished results). GaLV10A1 cell receptor is the Sodium-dependent phosphate transporter 1 (SLC20A1) protein [61]. HEK 293T SLC20A1 knock-out (KO) supported GaLV10A1$^{\Delta R}$ expression in transient settings without inducing syncytia formation (unpublished results). This opened the possibility to establish a constitutive LV producer cell line expressing this high-titer envelope glycoprotein.

1.7. Aim and strategy

The aim of this work was to evaluate the potential of the high-titer GaLV10A1$^{\Delta R}$ envelope glycoprotein for stable expression, in order to enable its use in constitutive LV producer cells. To this end, we used the previously established HEK 293T SLC20A1 KO cell line (unpublished results) as the starting cells of this work.

The first goal was to characterize HEK 293T SLC20A1 KO phenotype at the level of cell growth, LV productivity and resistance to syncytia formation. For the latter, we developed a new analytical method to quantify syncytia formation, based on cell size distribution. SLC20A1 KO phenotype was also evaluated through SLC20A1 complementation studies. The second goal was to establish new cell populations stably expressing GaLV10A1$^{\Delta R}$, as well as the original GaLV10A1 and the remaining GaLV10A1 derived envelope glycoproteins (GaLV10A^{pro} and GaLV10A1^{giflet}) and characterize them at the level of envelope glycoprotein expression and cell growth. The third and final goal was to evaluate the potential for LV production of the newly established cell populations.

2. Materials and methods

2.1. Plasmids

Primers and templates for all the plasmids constructed during this work are listed in **Table A.1.** A schematic representation of each plasmid and their main transcriptional units is provided in **Figure A.1**, in annexes.

2.1.1. Lentiviral vectors packaging plasmids

pMDLg/pRRE is a third-generation LV packaging plasmid expressing the Gag-Pro-Pol polyprotein from the HIV-1, under the control of the CMV promoter. It also contains a Rev responsive element (RRE), which is a binding site for the HIV-1 Rev protein that facilitates the export of RRE containing RNAs from the nucleus to the cytoplasm.

pRSV-Rev is a third-generation LV packaging plasmid encoding the second and third exons of HIV-1 *rev*, under the control of the Rous sarcoma virus (RSV) U3 promoter.

These plasmids were kindly provided by Dr. Didier Trono through Addgene plasmid repository (Cambridge, MA, USA, plasmids #12251 and # 12253, respectively) and are described in [33].

2.1.2. Lentiviral vector pseudotyping plasmids

pMD2.G is a plasmid coding for the G glycoprotein of vesicular stomatitis virus envelope (VSV-G) under the control of a CMV promoter, kindly provided by Dr. Didier Trono through Addgene plasmid repository (plasmid #12259).

pCMV-GaLV10A1 is a plasmid encoding the modified gibbon ape leukemia virus envelope glycoprotein (GaLV) and zeocin resistance marker under the transcriptional control of a CMV promoter. GaLV10A1 is a modified version of GaLV glycoprotein in which the cytoplasmatic tail was substituted by that of MLV 4070A envelope, as described in [56]. It also contains rabbit beta-globin (RBG) and hemoglobin subunit beta 2 (HBB2) introns upstream of *GaLV10A1* start codon. This plasmid was derived from *phGaLV10A1,* kindly provided by Dr. Otto Merten (Généthon, Évry, France), where the 19 nucleotides preceding galv10a1 start codon were removed by inverted PCR, as described in [62].

pCMV-GaLV10A1^{pro}, pCMV-GaLV10A1^{giflet} and pCMV-GaLV10A1$^{\Delta R}$ plasmids are *pCMV-GaLV10A1* derivatives and encode engineered versions of GaLV10A1 envelope glycoprotein regarding the sequence of R-peptide cleavage site: i) GaLV10A1^{pro} has its cleavage site sequence replaced by the HIV-1 matrix/capsid (MA/CA) cleavage site sequence (SQNY↓PIVQ) [59]; ii) GaLV10A1^{giflet} has its cleavage site sequence replaced by a synthetic cleavage site sequence (GSGIF↓LETSL) described in [60]; iii) GaLV10A1$^{\Delta R}$ has its R-peptide deleted from the 4070A cytoplasmic tail [63]. All these plasmids are described in [55].

pMonoZeo-GaLV10A1, pMonoZeo-GaLV10A1^{pro}, pMonoZeo-GaLV10A1^{giflet} and pMonoZeo-GaLV10A1$^{\Delta R}$ are plasmids coding for GaLV10A1, GaLV10A1^{pro}, GaLV10A1^{giflet} and GaLV10A1$^{\Delta R}$ envelope glycoproteins, respectively. These plasmids were derived from *pMonoZeo-4070A* [45], a construct expressing the MLV 4070A envelope glycoprotein, under the control of a composite promoter made of a SV40 enhancer and a ferritin heavy chain core promoter (SV40/FerH) and the 5' UTR of the mouse elongation factor 1 alpha gene (mEF1α). A zeocin resistance marker is also coupled to the envelope glycoprotein expression by a foot-and-mouth disease virus internal ribosome entry site (FMDV IRES). To construct *pMonoZeo-GaLV10A1* and its derivates, *4070A* envelope glycoprotein gene was removed by enzymatic restriction and replaced by *GaLV10A1*, *GaLV10A1^{pro}*, *GaLV10A1^{giflet}* and *GaLV10A1$^{\Delta R}$*, PCR amplified from *pCMV-GaLV10A1*, *pCMV-GaLV10A1^{pro}, pCMV-GaLV10A1^{giflet} and pCMV-GaLV10A1$^{\Delta R}$*, respectively.

From now on GaLV10A1, GaLV10A1^{pro}, GaLV10A1^{giflet} and GaLV10A1$^{\Delta R}$ envelope glycoproteins will be referred as GaLV, GaLVpro, GaLVgiflet and GaLVΔR, respectively.

2.1.3. Lentiviral vector transgenes

pRRLSIN.cPPT.PGK-GFP.WPRE is a self-inactivating (SIN) [36], third generation compatible [33] LV encoding the enhanced green fluorescence protein (eGFP) [64] under the control of an internal human phosphoglycerate kinase 1 (hPGK) promoter. This plasmid was kindly provided by Dr. Didier Trono through Addgene plasmid repository (plasmid #12252).

pRRLSIN-EF1α-SLC20A1-emcvIRES-Hygro-WPRE and *pRRLSIN-EF1α-SLC20A2-emcvIRES-Hygro-WPRE* are SIN third generation compatible LV encoding the Sodium-dependent phosphate transporter 1 (SLC20A1 also known as PiT-1) and Sodium-dependent phosphate transporter 2 (SLC20A2 also known as PiT-2) proteins, respectively, under the control of the elongation factor 1 alpha (EF1α) promoter, coupled to a hygromycin resistance marker (hygro^{R}) through an encephalomyocarditis virus internal ribosome entry site (EMCV IRES). These plasmids were derived from an in-house construct – pRRLSIN-EF1a-CRE-emcvIRES-Puro-WPRE [65] – where *cre* was removed by enzymatic restriction and replaced by *SLC20A1* or *SLC20A2*. *SLC20A1* and *SLC20A2* were amplified by PCR from *pDONR221* plasmids (clone ID: HsCD00045579 and HsCD00043621, respectively) acquired from DNASU Plasmid Repository (Biodesign Institute, Arizona State University, Tempe, AZ, USA). Puromycin resistance marker was then excised by enzymatic restriction and replaced by *hygro^{R}* amplified by PCR from *pREV-Hygro-WPRE* [45].

pRRLSIN-EF1α-mCherry-emcvIRES-Hygro-WPRE is a SIN third generation-associated lentiviral vector derived from *pRRLSIN-EF1α-SLC20A2-emcvIRES-Hygro-WPRE*, encoding a monomeric red fluorescence protein (mCherry [66]). *SLC20A2* sequence was removed by enzymatic restriction and replaced by *mcherry*. mCherry was PCR amplified from *pPuro_mCherry NheI*, an in-house plasmid encoding mCherry under the control of a human elongation factor 1 alpha/Human t-Cell Leukemia Virus (EF1a/HTLV) composite promoter.

From now on, SLC20A1 and SLC20A2 will be referred as PiT-1 and PiT-2, respectively.

2.1.4. Other plasmids

pRRLSIN.cPPT.PGK-GFP.WPRE_ALB is a SIN third generation associated-LV derived from *pRRLSIN.cPPT.PGK-GFP.WPRE,* encoding the human albumin (ALB) protein and an eGFP protein under the control of a hPGK promoter. The cDNA of human *ALB* was amplified by PCR from a *pDONR221* plasmid (clone ID: HsCD00043431) acquired from DNASU Plasmid Repository (Biodesign Institute) and cloned into *pRRLSIN.cPPT.PGK-GFP.WPRE* through In-Fusion® HD cloning Kit (Clontech Laboratories, Inc.) after being digested with KpnI restriction enzyme.

pCI-neo is a mammalian expression vector commercially acquired (Cat. #E1841, Promega Corporation, Madison, Wisconsin, USA) containing a multiple cloning site where a gene on interest can be placed under the control of a CMV immediate-early enhancer/promoter.

2.2 Cloning procedures

DNA amplification was done by PCR using Phusion® High-Fidelity DNA Polymerase (Finnzymes Oy, Vantaa, Finland), following the manufacturer instructions in a Biometria® T3 Personal Thermocycler (Biometria, Göttengen, Germany).

Each enzymatic restriction was performed using NEB® (New England Biolabs, Ipswich, MA, USA) restriction enzymes and buffers, according to the conditions suggested by the manufacturer.

PCR amplicons and restriction fragments were isolated using 0.7% (w/v) agarose gels (NZYTech, Lisbon, Portugal) stained with 0.5µL/mL RedSafe™ Nucleic Acid Stainng Solution (INtRON Biotechnology, South Korea) and visualized *using GelDoc™ XR⁺ system* (BioRad, Hercules, CA, USA). The resulting fragments were purified using NucleoSpin® Gel and PCR Clean-up Kit (Macherey-Nagel, Düren, Germany) according to the manufacturer instructions.

Cloning reactions were performed using In-Fusion® HD cloning Kit (Clontech Laboratories, Inc., Mountain View, CA, USA), following the manufacturer instructions.

2.3. Site directed mutagenesis

The site directed mutagenesis protocol used in this work, described in [67], was performed using Phusion® High-Fidelity DNA Polymerase (Finnzymes Oy), 5'-phosphorylated primers for DNA amplification, DpnI restriction enzyme for template DNA digestion and T4 DNA Ligase (New England Biolabs) for PCR product circularization, according to the manufacturer instructions.

2.4. Bacterial strains and culture media

Escherichia coli Stellar™ (Clontech Laboratories, Inc.) competent bacteria were used for cloning reactions and plasmid amplification. *Escherichia coli* One Shot® STBL3™ (Invitrogen™, Carlsbad, CA, USA),

Max Efficiency™ DH5α (Invitrogen™) and Neb® Stable (New England Biolabs) competent bacteria were used for plasmid amplification.

Liquid and agar cultures were performed using Luria Broth (LB) media (Fast-Media® LB, Invivogen, San Diego, CA, USA) and Terrific Broth (TB) media (Fast-Media® TB, Invivogen), supplemented with the appropriate antibiotic for bacteria selection (ampicillin, zeocin, kanamycin). Media was prepared following the manufacturer instructions, using ultrapure water (Milli-Q®, Merck Millipore, Billerica, MA, USA).

2.5. Plasmid purification and quality control

Plasmid purification was performed at small-scale using GeneJET Plasmid Miniprep Kit (Thermo Scientific™, Waltham, MA, USA) and at larger scale using Genopure Plasmid Maxi Kit (Roche Applied Science, Penzberg, Germany) according to the manufacturer instructions. Bacteria banks for each new plasmid were generated and stored at -80º C with 15% of glycerol (Sigma-Aldrich, St. Louis, MO, USA).

DNA and RNA concentration were assessed using *Nanodrop™ 2000 Spectrophotometer* (Thermo Scientific™) and their purity was determined by measuring Abs_{260nm}/Abs_{280nm} and Abs_{260nm}/Abs_{230nm} ratios.

Every new plasmid developed was sequenced by Sanger sequencing, using Eurofins Scientific services (Brussels, Belgium).

2.6. Cell lines and culture conditions

HEK 293T (ATCC, American Type Cell Collection, CRL-3216), is a cell line derived from the Human Embryonic Kidney 293 (HEK 293) cell line, constitutively expressing the SV40 large T antigen [68], from now it will be referred as 293T cells.

HEK 293T Cas9 is a Human Embryonic Kidney 293T derived cell line constitutively expressing Cas9 endonuclease. This cell line was established (unpublished results) by transducing HEK 293T cells with lentiviral vectors harbouring the lentiCas9-Blast transgene from the Dual-vector lentiviral Genome-scale Knock-out (GeCKO) system described in [69], from now it will be referred as 293T Cas9 cells.

HEK 293T SLC20A1 Knock-out (KO) clone 3.4 is a Human Embryonic Kidney 293T cell line were the Sodium-dependent phosphate transporter 1 (SLC20A1) protein, known to be the Gibbon ape leukemia virus cell receptor [61,70], was deleted by CRISPR-Cas9 genome editing. This cell line was established (unpublished results) by transducing HEK 293T cells with LV harbouring the lentiCRISPRv2 transgene from the Single-vector lentiviral GeCKO system, described in [69], using three different single guide RNAs (sgRNA) (**Table A.2**), from now it will be referred as 293T PiT-1 KO cells.

HEK 293 FLEX S11 cell line is a HEK 293 derived cell line stably producing MLV based recombinant retroviral vectors, pseudotyped with GaLV envelope glycoprotein, as described in [71]. These cells were used as a positive control for GaLV protein quantification. From now on only referred as 293 FLEX S11 cells.

All cells were cultured in Dulbecco's modified Eagle's medium (DMEM, Corning Inc, Corning, NY, USA) supplemented with 10% (v/v) Fetal Bovine Serum (FBS, Gibco), and maintained at 37º C, in a humidified atmosphere of 8% (v/v) CO_2. Cells were cultured in tissue culture flasks (T-flask, Starstedt, Numbrecht, Germany) under adherent conditions.

Working cell banks were established by freezing cells in FBS containing 10% (v/v) of Dimethyl Sulfoxide (DMSO, Sigma-Aldrich, St. Louis, MO, USA) and stored at -80º C.

2.7. Cell concentration and viability

Cell concentration and viability assessment was based on the trypan blue exclusion assay, using a 0.1% (v/v) Trypan Blue (Sigma-Aldrich) solution in Phosphate-Buffered Saline (PBS) (Gibco™). Cell counting was performed using a Fuchs-Rosenthal hemocytometer (Marienfield-Superior, Lauda-Konigshofen, Germany) on an inverted microscope (Olympus, Tokyo, Japan).

2.8. Adherent cell transfection procedure

For syncytia quantification method (section 2.9) and for establishing new cell lines for stable expression of GaLV engineered envelope glycoproteins (section 2.10.1), an adherent cell transfection protocol was used. To this end, cells were seeded at a concentration of $5x10^4$ cells/cm^2. Cell transfection was performed 24 hours after seeding using polyethylenimine (PEI, Linear 25kDa, Polysciences, Inc., Warrington, PA, USA) as transfection reagent, in a 1:1.5 (w/w) ratio of DNA:PEI. Transfection was carried with a total of 5 µg of DNA per million of cells. DNA mix was added to the PEI transfection mix, after being filtered through a 0.22 µm pore-size cellulose acetate filter, both prepared in serum-free DMEM. After a period of incubation of 12 minutes, at room temperature, the final transfection mix was added to the cells.

2.9. Syncytia quantification method

Cells were transfected with *pMonoZeo-GaLV10A1* or *pMonoZeo-GaLV10A1$^{\Delta R}$* as described in section 2.8. Cells were harvested 48 hours post-transfection and analysed by flow cytometry (CyFlow® Space, Sysmex Corporation, Kōbe, Japan) or by an image-based cell analyser (Cedex HiRes Analyzer, Roche Applied Science). Non-transfected cells were used as negative controls. Data obtained with flow cytometry was analysed using FlowJo™ software and data obtained by Cedex HiRes Analyzer was analysed using R software [72].

2.10. Cell line development

2.10.1. Stable expression of engineered envelope glycoproteins

293T and 293T PiT-1 KO were used to establish several cell populations constitutively expressing GaLV envelope glycoprotein or its engineered versions (GaLVpro, GaLVgiflet and GaLVΔR). To this end, cells were transfected as described in section 2.8, in 6-well plates, with *pMonoZeo-GaLV10A1, pMonoZeo-GaLV10A1^{pro}, pMonoZeo-GaLV10A1^{giflet}* or *pMonoZeo-GaLV10A1$^{\Delta R}$*. At 48 hours post-transfection, cells were

harvested and transferred into a 25 cm^2 t-flask. Cell selection was conducted using fresh culture medium supplemented with 200 µg/mL of Zeocin (Invivogen), through regular medium exchange.

2.10.2. 293T PiT-1 KO: complementation studies

293T Cas9 and 293T PiT-1 KO were transduced with LV harbouring one of three different transgenes (*PiT-1*, *PiT-2* and *mcherry*) encoded in a *pRRLSIN-EF1α-GOI-emcvIRES-Hygro-WPRE* backbone. Cell transduction was performed at the moment of seeding, using an inoculum of $5x10^4$ cells/cm^2, in 6 well plates, in a final volume of 1 mL containing 8 µg/mL polybrene (Sigma-Aldrich). Cells were transduced with a multiplicity of infection (MOI) of 2.5 infectious particles per cell. Fresh culture media was added to the cells at 4 hours post-transduction. At 72 hours post-transduction, cells were transferred into a 75 cm^2 t-flask. Cell selection was conducted using fresh culture medium supplemented with 200 µg/mL of Hygromycin (Invivogen), through regular medium exchange.

2.11. Lentiviral vector production

Transient LV production was performed using a third-generation lentiviral packaging system described in [33]. 293T, 293T Cas9 or 293T PiT-1 KO, were seeded at a concentration of $1.5x10^5$ cells/cm^2, and transfected at the moment of seeding – transfection at seeding protocol – with a total of 3.3 µg of plasmid DNA per million cells with the following proportions: 0.7 µg of *pMDLg/pRRE*, 0.2 µg of *pRSV-Rev*, 0.6 µg of envelope plasmid and 1.8 µg of LV transgene plasmid. PEI (Polysciences, Inc.) was used as transfection reagent, at a 1:1.5 (w/w) ratio of DNA:PEI. Both plasmid DNA mix and PEI solution were prepared in serum-free DMEM. Plasmid mix was filtered through a 0.22 µm pore-size cellulose acetate filter and then added to the PEI solution. The transfection mix was incubated for 12 minutes, at room temperature and then added to the cell suspension. At 24 hours post-transfection, the culture medium was exchanged by DMEM supplemented with 10% (v/v) FBS. The LV containing supernatant was harvested 24 hours later, clarified through a 0.45 µm pore-size cellulose acetate filter, aliquoted and stored at -80º C until further use. Transfection efficiency was accessed by measuring the percentage of GFP positive cells at 48 hours post-transfection by flow cytometry (CyFlow® Space).

2.12. Lentiviral vector titration

2.12.1. Lentiviral vector titration by Flow Cytometry

To determine infectious particles titers, 293T cells were seeded in 24-well plates at $8x10^4$ cells/cm^2. Cells were transduced 24 hours after seeding with several dilutions of lentiviral supernatant in fresh medium containing polybrene (Sigma-Aldrich), at a final concentration of 8 µg/mL. Plates were then centrifuged for 2 hours, at 1200 x g, 25º C. After centrifugation, 0.5 mL of DMEM supplemented with 10% (v/v) FBS was added to each well. At 48 hours post transduction, the percentage of GFP positive cells was determined by flow cytometry (CyFlow® Space). Infectious particles titer per millilitre (I.P./mL) was calculated by considering the

number of cells at the moment of transduction, the percentage of GFP positive cells, the lentiviral supernatant dilution and the volume of infection, according to the following equation:

$$\frac{I.P.}{mL} = \frac{\%\ GFP\ positive\ cells\ \times numbers\ of\ cells\ at\ infection\ \times dilution\ factor}{100 \times infection\ volume\ (mL)}$$

Only lentiviral dilutions that yielded percentages of GFP positive cells between 2% to 20% were used to determine infectious particles titers.

2.12.2. Titration by vector copy *per* nucleus qPCR (VCN-qPCR)

LV harbouring *PiT-1* or *PiT-2* transgenes (from *pRRLSIN-EF1α-SLC20A1-emcvIRES-Hygro-WPRE* and *pRRLSIN-EF1α-SLC20A2-emcvIRES-Hygro-WPRE* plasmids, respectively) used to complement 293T PiT-1 KO were titered was performed using a vector copy *per* nucleus (VCN) qPCR titration method, since *PiT-1* and *PiT-2* transgenes do not carry reporters. This method determines the number of integrated LV genomes by quantitative PCR directly from transduced cell lysates, using the human *ALB* as an internal reference gene.

293T cells were seeded in 24-well plates at $8x10^4$ cells/cm^2. Cells were transduced 24 hours after seeding with several dilutions of lentiviral supernatant in fresh medium containing polybrene (Sigma-Aldrich), at a final concentration of 8 µg/mL. At 48 hours post transduction, cell extracts were prepared by adding 100 µL of lysis buffer from Global UltraRapid Lentiviral Titering Kit (System Bioscience, Palo Alto, CA, USA) to each cell well followed by freezing at –80º C for at least 30 minutes. After thawing, extracts were heated at 95º C, for 10 minutes, followed by centrifugation at 1200 x g, for 5 minutes. Prior to centrifugation, the supernatants were aliquoted and stored at -20º C, until further use.

The detection of integrated LV genomes and reference gene was done by Multiplex qPCR using LightCycler 480 Probes Master mix (Roche Applied Science), ALB TaqMan Copy Number Assays (Thermo Scientific) primer/probe mix, LTR probe (IDT, Coralville, Iowa, USA) and primers. The LTR probe was conjugated to HEX dye at 5' end and the Iowa BLACK® Quencher at 3' end. The ALB probe (undisclosed sequence), integrated in the commercially acquired mix, was labelled with FAM dye. LTR primers and probe sequences are listed in **Table A.3**.

Calibration curves were established with 10-fold serial dilutions of the dual plasmid *pRRLSIN.cPPT.PGK-GFP.WPRE_ALB,* which contains the LTR and *ALB* sequences, ranging from $1x10^8$ to $1x10^2$ copies/µL. These calibration curves were used to establish a linear regression which correlates the cycle threshold (Ct) values with known concentrations of the standard plasmid. These linear regressions were used to calculate the number of copies/µL of the LTR and *ALB* sequences in each sample, based on their Ct values.

VCN were determined by correlating the number of integrated LV sequences to the number of *ALB* (reference), using the following equation:

$$VCN = \frac{\frac{copies}{\mu L}\ LV\ sequence}{\frac{copies}{\mu L}\ reference}\ x\ N$$

where "N" indicates the number of genomic copies of the reference gene *per* cell genome.

LV titers, in transducing units per mL (T.U./mL), were determined using the following equation:

$$\frac{T.U.}{ml} = \frac{VCN\ x\ C\ x\ D}{V}$$

Where "C", "D" and "V" indicate the number of cells at infection, the LV supernatant dilution and the volume of LV supernatant (in mL) used for transduction, respectively.

2.13. RNA extraction and cDNA synthesis

Total cellular RNA extraction was performed using QIAamp® RNeasy Mini Kit (Qiagen, Hilden, USA) according to the manufacturer instructions. After extraction, RNA was quantified using *Nanodrop™* 2000 Spectrophotometer (Thermo Scientific™) and stored at -80º C until further use.

cDNA synthesis was performed using Transcriptor High Fidelity cDNA Synthesis Kit (Roche Applied Science) according to manufacturer instructions. Anchored Oligo(dT)$_{18}$ primer and 2 µg of total RNA were used for total mRNA reverse transcription and the synthetized cDNA was stored at -20º C, until further use.

2.14. Real-Time quantitative PCR for quantitative gene expression

The mRNA levels of the different envelope glycoproteins was assessed by Real-Time quantitative PCR (RT-qPCR) using the $2^{-\Delta CT}$ method [73], using the ribossomal protein L22 (*RPL22*) gene as reference. RT-qPCR was performed using LightCycler® SYBR Green I Master (Roche applied Science) according to the manufacturer instructions, in a LightCycler® 480 Real Time PCR System (Roche Applied Science). Primer sequences (forward and reverse) used for RT-qPCR are listed in **Table A.3**, in annexes.

2.15. Complementation studies

To probe a potencial cause-effect relation between PiT-1 deletion and the absence of syncytia formation, PiT-1 KO complemented cell populations (section 2.10.2) were transfected with *pMonoZeo-GaLV10A1* and *pMonoZeo-GaLV10A1$^{\Delta R}$* as described in section 2.8. Cells were harvested at 48 hours post-transfection and syncytia formation was quantified using an image-based cell analyser (Cedex HiRes Analyzer, Roche Applied Science) as described in section 2.9.

2.16. Cell growth studies and specific growth rate

To evaluate cell growth of 293T PiT-1 KO cell line, of the newly established cell populations stably expressing GaLV engineered envelope glycoproteins and of the cell populations established in the PiT-1

complementation studies, cells were seeded at a concentration of 2 x 10^4 cells/cm^2, in 25 cm^2 tissue culture flasks. Cells were counted and their viability was accessed for the next 7 days (every 12 hours between the second and the sixth day after seeding) using an image-based cell analyser (Cedex HiRes Analyzer, Roche Applied Science). 293T, 293T Cas9 cell lines were used as cell growth controls.

Specific growth rates (μ), given the inicial number of individuals (C_0) at an inicial time point (t_0) and the number of individuals C_x at the time point t_x were determined according to the following equation:

$$C(x) = \mu . \int_{t_0}^{t_x} C . dt$$

A confidence interval of 95% was considered in these calculations.

2.17. Protein extraction

For total protein extraction 3 x 10^6 cells were pelleted at 300 x g, for 10 minutes, washed with PBS, re-pelleted and resuspended in 100 μL of lysis solution [Mammalian Protein Extraction Reagent (M-PER, Thermo Scientific™) supplemented with cOmplete™ EDTA-free Protease Inhibitor Cocktail (Roche Applied Science)]. The resuspended cells were homogenised by vortexing for 5 seconds and incubated on ice, for 2 minutes, followed by vortexing for 5 seconds and a new incubation period on ice, for 2 minutes. Protein extracts were clarified by centrifugation, 14000 x g for 10 minutes, and stored at -80º C until further use.

2.18. Protein quantification

2.18.1. PiT-1 and PiT-2 quantification by western blot

PiT-1 and PiT-2 protein expression levels in 293T PiT-1 KO cell line and in the cell populations established in the PiT-1 complementation study (section 2.15), were evaluated by western blotting.

Total protein quantification was performed using Pierce™ BCA Protein Assay Kit (Thermo Scientific™), as described by the manufacturer.

Protein electrophoresis was performed using NuPAGE® electrophoresis system (Life Technologies™, Carlsbad, CA, USA). Protein separation was performed under denaturing conditions, in a NuPAGE® 4-12% Bis-Tris gel with MOPS SDS Running Buffer, at 180 V, for 50 minutes, as described by the manufacturer. The resolved protein samples were transferred into nitrocellulose membranes using the iBlot® Transfer Stack kit (Invitrogen™), in a iBlot® Dry Blotting System (Invitrogen™), according to the manufacturer instructions. After protein transfer, the nitrocellulose membranes were blocked in a Tris-Buffered Saline solution (TBS, Sigma-Aldrich) with 0.1% (v/v) Tween 20 (Sigma-Aldrich) and 5% (w/v) skim milk powder (Sigma-Aldrich) for 1 hour, at room temperature, and incubated overnight with primary antibody. PiT-1 and PiT-2 detection was performed using mouse anti-PiT-1 (LOM-C39175-50, LabOmics) and rabbit anti-PiT-2 (LOM-C80492-50, LabOmics), diluted 1:1000 and 1:500, respectively, in TBS with 0.1% (v/v) Tween 20 and 5% (w/v) Bovine

Serum Albumin (Sigma-Aldrich). The nitrocellulose membranes were washed 3 times in a washing solution of TBS 0.1% (w/v) Tween 20 and incubated with secondary antibody, at room temperature, for 2 hours with gentle agitation. ECL™ Anti-mouse IgG (NA931VS) or ECL™ anti-rabbit IgG (NA934VS) Horseradish peroxidase-conjugated antibodies (GE Healthcare, Little Chalfont, UK) were used as secondary antibodies, diluted 1:5000 in blocking solution. After incubation, membranes were washed 3 times in washing solution and Chemiluminescence detection was performed using the Amersham™ ECL™ prime western blotting detection reagent kit (GE Healthcare), as described by the manufacturer, in a ChemiDoc XRS System (Bio-Rad). Alpha-tubulin was chosen as loading control (mouse anti-alpha-tubulin, T6199, Sigma-Aldrich, diluted 1:5000).

2.18.2. Staining of cell surface GaLV envelope glycoprotein

To evaluate constitutive expression of GaLV envelope glycoprotein (or its derivates), envelope glycoprotein at cell surface was quantified by immunofluorescence in live cells. To this end, cells were harvested and pelleted at 800 x g for 2 minutes, in V-shaped 96 well plates (0.2 million cells per well). After washing with PBS with 2% FBS (v/v), cells were stained using an antibody against GaLV envelope glycoprotein, mouse anti-GaLV IgG2a (cat ID. LOM-00J004, LabOmics, Nivelles, Belgium), diluted 1:10 in PBS with 2% (v/v) FBS (incubated for 1 hour, at 4º C). After staining with primary antibody, cells were washed 3 times with PBS with 2% (v/v) FBS and then incubated with secondary antibody, Alexa Fluor® 488 Goat anti-mouse IgG (cat ID. A11001, Invitrogen™), diluted 1:100 in PBS with 2% (v/v) FBS, for 30 minutes, at 4º C. Stained cells were washed 3 times with PBS with 2% (v/v) FBS and the percentage of GaLV positive cells and mean fluorescence intensity was determined by flow cytometry (CyFlow® Space).

3. Results

The aim of this work was to evaluate the potential of the high-titer GaLVΔR envelope glycoprotein [55] for stable expression, in order to enable its use in constitutive LV producer cells. To accomplish this objective, the work was based on 293T PiT-1 KO, previously shown to cope with this envelope cytotoxicity in transient expression studies. Focusing on this cell line, this project was divided in three lines of work: i) phenotype characterization; ii) stable expression of GaLV envelope glycoproteins and iii) semi-stable LV production. 293T and 293T Cas9 (stably expressing Cas9 endonuclease) cell lines were used as controls and/or terms of comparison throughout the entire work.

3.1. 293T PiT-1 KO phenotype characterization

Before 293T PiT-1 KO could be used to establish new cell populations constitutively expressing envelope glycoproteins and, ultimately, develop a stable producer cell line, they were characterized to evaluate the impact of PiT-1 deletion on cell growth, LV production and resistance to syncytia formation.

3.1.1. Cell growth

293T PiT-1 KO cells seem to present a similar morphology to 293T and to 293T Cas9 cells (**Figure 3.1**). We evaluated the impact of PiT-1 deletion on cell growth (**Table 3.1 and Figure 3.2**).

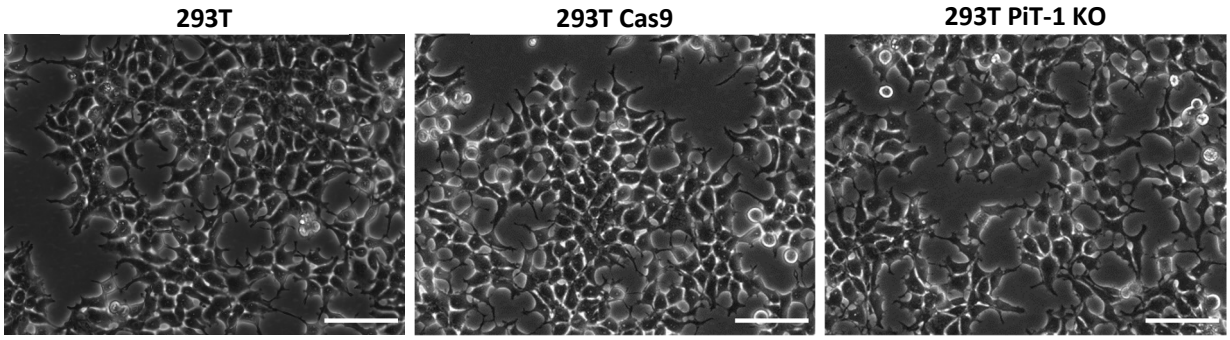

Figure 3. 1 – Cell morphology of 293T, 293T Cas9 and 293T PiT-1 KO cell lines. Images obtained by phase-contrast microscopy. Scale bar: 100 µm.

The growth rate of 293T PiT-1 KO was lower than that of 293T and 293T Cas9 (**Table 3.1** and **Figure 3.2 A**). These cells also achieved lower maximum cell density (less than half) when compared to 293T (**Figure 3.2 A**). Relatively to cell viability, both 293T PiT-1 KO and 293T Cas9 had their viability greatly reduced much earlier than 293T (**Figure 3.2 B**).

Table 3. 1 – Specific cell growth rates of 293T, 293T Cas9 and 293T PiT-1 KO

Cell line	Specific growth rate (h^{-1})
293T	0.035±0.002
293T Cas9	0.037±0.003
293T PiT-1 KO	0.030±0.002

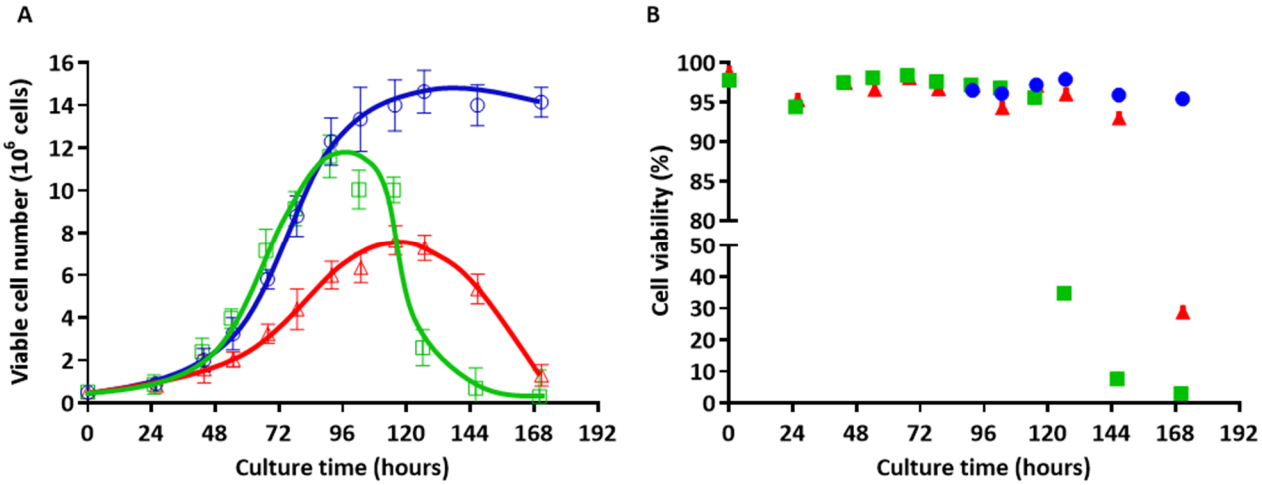

Figure 3. 2 – Impact of PiT-1 deletion on cell growth. Cell growth (A) and viability (B) of 293T PiT-1 KO cell relatively to the control cell lines 293T and 293T Cas9. Values are shown as 10^6 viable cells per t-flask (25 cm^2) and error bars correspond to the standard deviation associated to each cell count on the Cedex HiRes analyser. Blue, green and red colours represent 293T (●), 293T Cas9 (■) and 293T PiT-1 KO (▲) cell lines, respectively.

3.1.2. Lentiviral vector production

To evaluate the impact of Pit-1 deletion in LV productivity, we performed transient LV production with different envelope glycoproteins: VSV-G, GaLV and GaLVΔR. The results showed that, for each envelope glycoprotein being used, LV titers were similar for all cell lines (**Figure 3.3**).

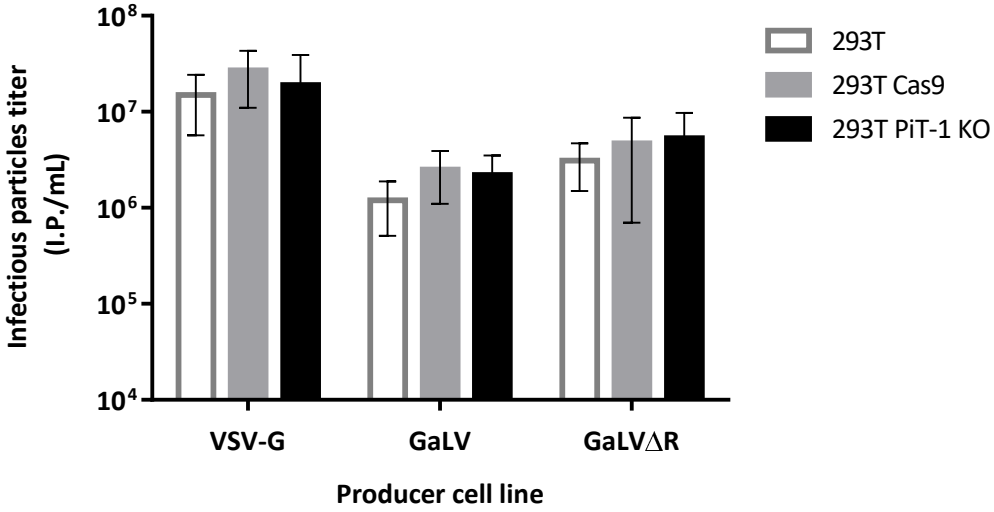

Figure 3. 3 – Impact of PiT-1 deletion in transient lentiviral vector production. Evaluation of the impact of PiT-1 deletion in LV titers pseudotyped with different envelope glycoproteins. Infectious particles titers (I.P./mL) are shown as average ± standard deviation of six biological replicates. No significant differences in LV titers were observed between cell lines given by a two-tailed, non-paired t-test at a significance level of $p < 0.05$.

3.1.3. Syncytia formation

293T PiT-1 KO cell line was established with the main purpose of enabling stable expression of GALVΔR without leading to the formation of syncytia. Syncytia are evident by microscopy analysis (**Figure 3.4**). 293T PiT-1 KO transfected with GaLVΔR do not exhibit syncytia formation in contrast with 293T or 293T Cas9. GaLV did not lead to syncytia formation in any of the cell lines (**Figure 3.4**).

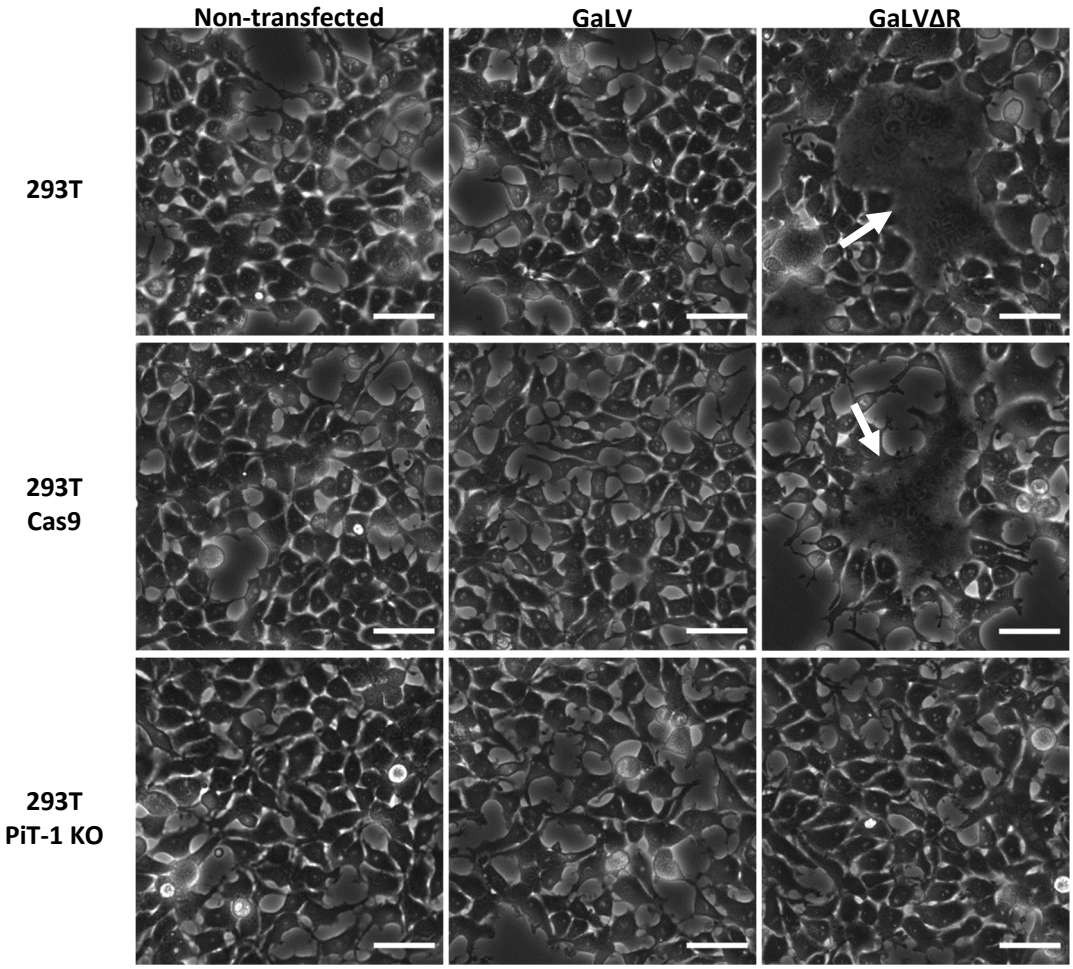

Figure 3. 4 – Syncytia formation with GaLVΔR envelope glycoprotein. 293T, 293T Cas9 and 293T PiT-1 KO were transfected with GaLV (control) or GaLVΔR envelope glycoproteins to evaluate syncytia formation. Non-transfected cells were used as negative control. Images obtained by phase contrast microscopy. Scale bar: 50 µm. White arrows indicate syncytia formation.

To complement microscopy data and obtain quantitative evidences on the abolishment of syncytia formation phenotype by PiT-1 KO, an analytical method based on cell size distribution was developed. In a first assay, transfected cells were analysed by flow cytometry (CyFlow® Space, Sysmex Corporation). However, the results showed no major differences in cell size distribution (data not shown).

In a second study the same analysis was performed using an image-based cell analyser (Cedex HiRes Analyzer, Roche Applied Science), followed by statistical analysis. To analyse cell size distribution data, we determined the maximum cell size observed in non-transfected cells. Then, we assessed the percentage of events with dimensions above this threshold, in cells expressing GaLV or GaLVΔR (**Table 3.2** and **Figure 3.5**).

The results showed that both 293T and 293T Cas9 cells expressing GaLVΔR had a much higher percentage of events above the maximum size threshold than cells expressing GaLV. For 293T PiT-1 KO, the percentage of events above the non-transfected control was minimal and equal between cells transfected with either GaLV or GaLVΔR (**Table 3.2**). Additionally, cell size distribution data analysis showed that, regardless of the envelope glycoprotein being expressed, 293T PiT-1 KO had a similar cell size distribution profile. This contrasted with 293T and 293T Cas9 where GaLVΔR transfected cells presented a different cell size distribution pattern when compared to GaLV transfected cells (**Figure 3.5**).

Table 3. 2 – Syncytia quantification method based on cell size distribution

Cell line		Maximum size (µm)[a]	Events above maximum size (%)[b]
293T	Non-transfected	75	-
	GaLV	95	1.0
	GaLV1ΔR	134	6.9
293T Cas9	Non-transfected	81	-
	GaLV	76	0.0
	GaLVΔR	190	14.0
293T PiT-1 KO	Non-transfected	89	-
	GaLV	94	0.2
	GaLVΔR	98	0.2

[a] Maximum event size detected using Cedex HiRes Analyser. [b] Percentage (%) of events with size above the non-transfected maximum.

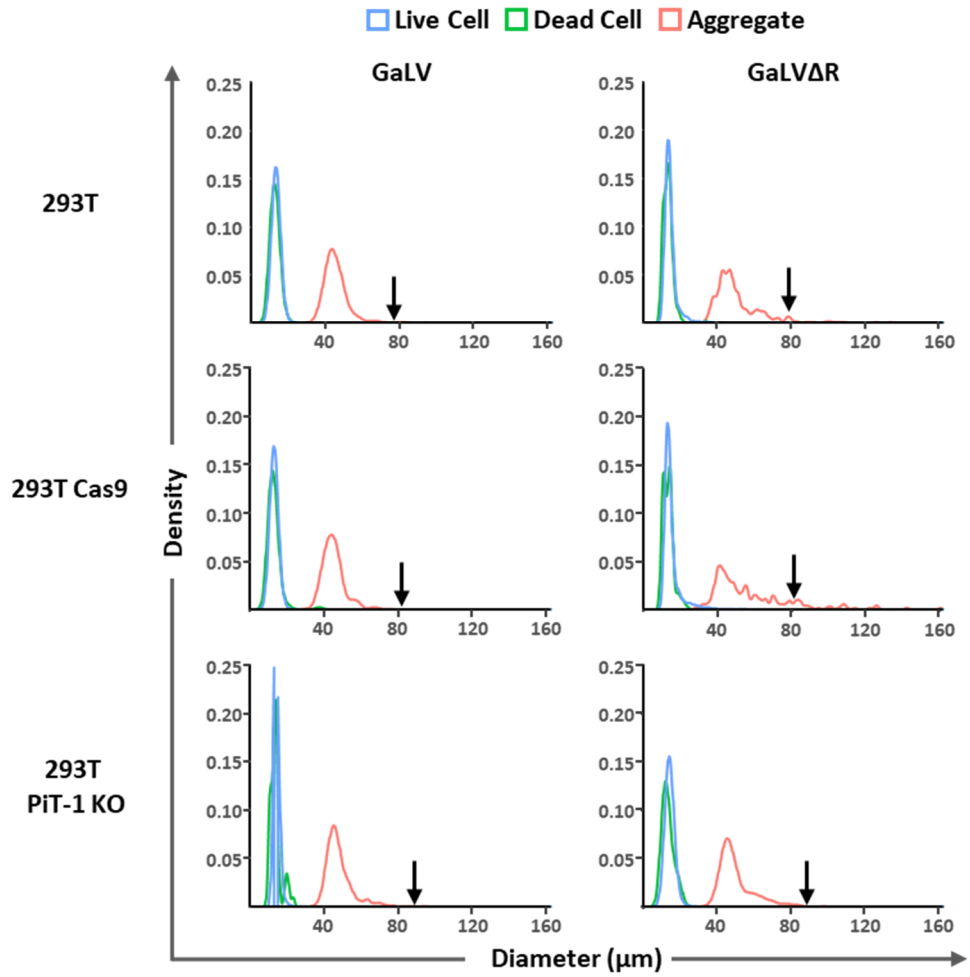

Figure 3. 5 – Syncytia quantification method based on cell size distribution. 293T, 293T Cas9 and 293T PiT-1 KO cell lines were transfected with GaLV or GaLV1ΔR envelope glycoproteins. Data was obtained using Cedex HiRes Analyser and treated with R software for density curve generation using a Kernel-based smoothing [74]. Non-transfected cells were used as negative control (not shown). Black arrows indicate the maximum event size detected in the respective non-transfected cells.

3.1.4. PiT-1 complementation study

To probe a potential cause-effect relation between PiT-1 deletion and the absence of syncytia formation or slower growth rate in 293T PiT-1 KO, we set to revert the KO phenotype by complementing these cells with PiT-1. In addition, PiT-2 and mCherry overexpression were used as controls.

After establishing the 293T Cas9 and 293T PiT-1 complemented cell populations the expression levels of PiT-1 and PiT-2 were assessed. PiT-1/PiT-2 expression was assessed by RT-qPCR and western blotting. mRNA and protein expression were also quantified in 293T, 293T Cas9 and 293T PiT-1 KO non-complemented cells as comparison.

The results from *PiT-1* gene expression showed that, every 293T PiT-1 KO cells (non-complemented, expressing mCherry, or complemented with PiT-2) presented on average a 8-fold decrease in mRNA levels, when compared to the 293T, further corroborating the PiT-1 KO phenotype. PiT-1 complementation in 293T PiT-1 KO cells not only rescued *PiT-1* mRNA levels, they registered a 20-fold increase in mRNA levels in

comparison to 293T (**Figure 3.6 A**). Relatively to 293T Cas9, PiT-1 complementation led to a 59-fold increase in mRNA levels when compared to non-complemented 293T Cas9. The remaining 293T Cas9 complemented cells (mCherry and PiT-2) showed *PiT-1* mRNA levels similar to 293T or 293T Cas9 cells (**Figure 3.6 A**).

The results from *PiT-2* gene expression showed that PiT-2 complementation in 293T Cas9 and 293T PiT-1 KO resulted in an approximate 108-fold increase in *PiT-2* mRNA levels comparatively to the non-complemented 293T Cas9 an 293T PiT-1 KO. Apart from these two, all the other cell lines exhibited low levels of *PiT-2* mRNA (**Figure 3.6 B**).

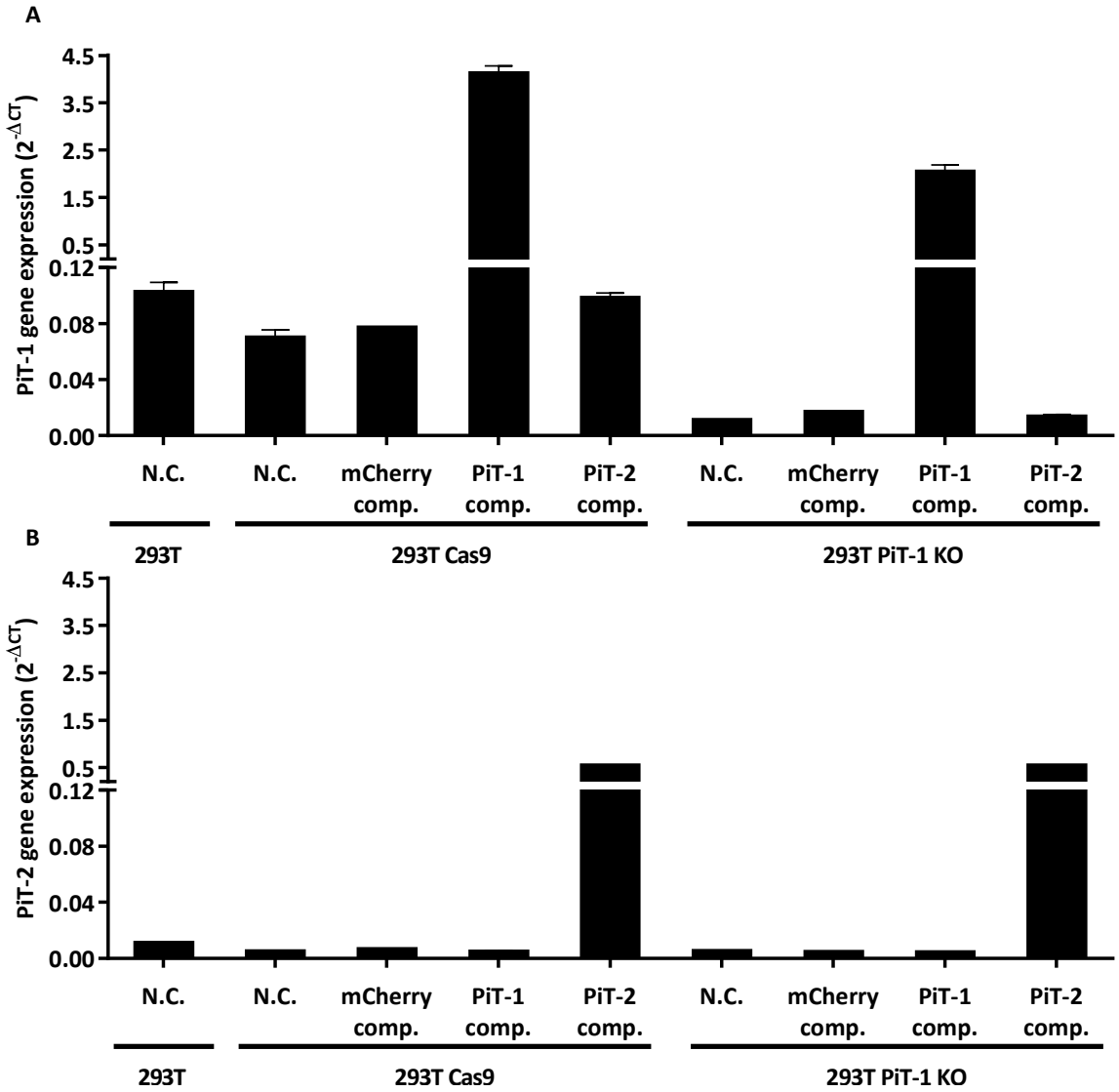

Figure 3. 6 – Comparison of *PiT-1* and *PiT-2* mRNA levels before and after complementation. *PiT-1* (**A**) and *PiT-2* (**B**) mRNA levels in non-complemented (N.C.) 293T, 293T Cas9 and 293T PiT-1 KO, in comparison to the 293T Cas9 and 293T PiT-1 KO complemented (comp.) cell populations stably expressing mCherry, PiT-1 and PiT-2. Gene expression was quantified using the $2^{-\Delta CT}$ method, after normalization to *RPL22* gene (control gene). Gene expression values are shown as average ± standard deviation of two technical replicates.

The protein expression analysis by western blotting showed similar levels of PiT-2 protein expression in all cell lines (**Figure 3.7**). Relatively to PiT-1 protein expression levels, the results were inconclusive since the expected band at 70.4 kDa was not observed in any cell line. Instead, a smaller band with approximately

50 kDa was detected in all samples (**Figure 3.7**). Two different anti-PiT-1 primary antibodies were tested, however, similar results were obtained (data not shown).

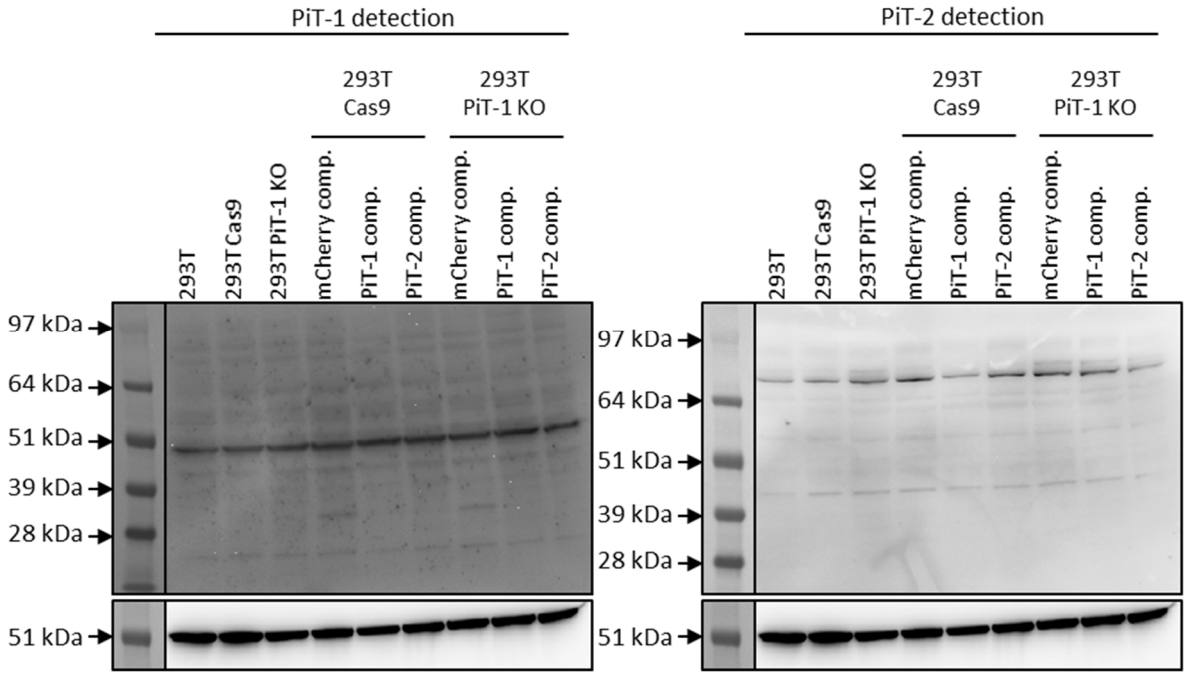

Figure 3. 7 – PiT-1 and PiT-2 protein expression in different cell lines. Western blot analysis of PiT-1 (73.7 kDa) and PiT-2 (70.4kDa) protein expression in 293T Cas9 and PiT-1 KO cell populations stably expressing mCherry (mCherry comp.), PiT-1 (PiT-1 comp.) and PiT-2 (PiT-2 comp.) proteins. Protein expression levels were also determined in 293T, 293T Cas9 and 293T PiT-1 KO cell lines as term of comparison. Protein extracts were analysed by immunoblotting with anti-PiT-1 and anti-PiT-2 antibodies.

After analysing PiT-1 and PiT-2 expression levels, we evaluated the growth profile of the different cell populations. Cell growth studies revealed that 293T Cas9 cells overexpressing either PiT-1 or PiT-2 had similar cell growth and viability relatively to mock control stably expressing mCherry and the non-complemented 293T Cas9 (**Table 3.3** and **Figure 3.8**). In other words, the overexpression of these receptors did not change the growth profile of non-KO cells. On the other hand, 293T PiT-1 KO cells experienced an increase in cell growth from either PiT-1 or PiT-2 overexpression (**Table 3.3** and **Figure 3.9 A**). However, this improvement did not revert the early drop in cell viability already seen in the first growth study (**Figure 3.9 B**).

Table 3. 3 – Specific cell growth rates of 293T Cas9 and 293T PiT-1 KO complemented cell populations

Cell line	Complementation	Specific growth rate (h^{-1})
293T Cas9	Non-complemented	0.037±0.003
	mCherry	0.034±0.003
	PiT-1	0.034±0.004
	PiT-2	0.033±0.003
293T PiT-1 KO	Non-complemented	0.030±0.002
	mCherry	0.033±0.002
	PiT-1	0.038±0.002
	PiT-2	0.036±0.001

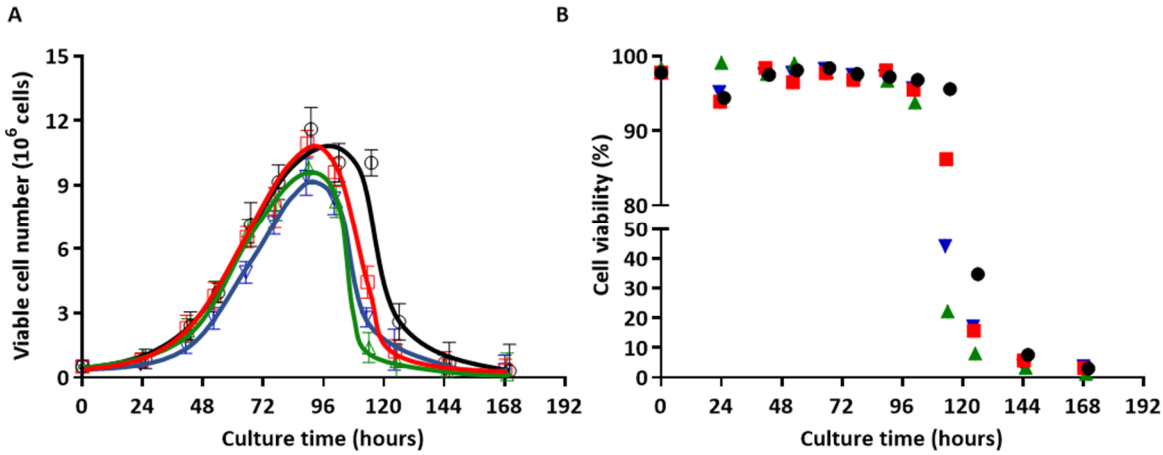

Figure 3. 8 – Impact of PiT-1 or PiT-2 overexpression in the growth profile of 293T Cas9 cells. Cell growth (A) and viability (B) of 293T Cas9 overexpressing mCherry, PiT-1 and PiT-2. Values are shown as 10^6 viable cells per t-flask (25 cm^2) and error bars correspond to the standard deviation associated to each cell count on the Cedex HiRes analyser. Red, green and blue colours represent 293T Cas9 stably expressing mCherry (■), PiT-1 (▲) and PiT-2 (▼), respectively. 293T Cas9, in black (●), were used as term of comparison.

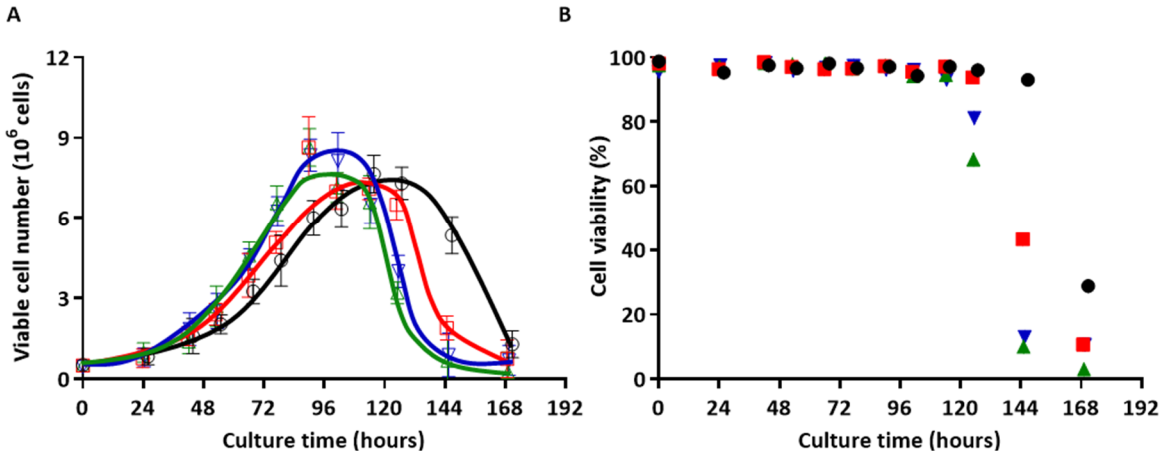

Figure 3. 9 – Impact of PiT-1 or PiT-2 overexpression in the growth profile of 293T PiT-1 KO cells. Cell growth (A) and viability (B) of 293T PiT-1 KO overexpressing mCherry, PiT-1 and PiT-2. Values are shown as 10^6 viable cells per t-flask (25 cm^2) and error bars correspond to the standard deviation associated to each cell count on the Cedex HiRes analyser. Red, green and blue colours represent 293T Cas9 stably expressing mCherry (■), PiT-1 (▲) and PiT-2 (▼), respectively. 293T PiT-1 KO, in black (●), were used as terms of comparison.

Finally, to probe a potencial cause-effect relation between PiT-1 deletion and the absence of syncytia formation, 293T Cas9 and 293T PiT-1 KO cell populations stably expressing mCherry, PiT-1 and PiT-2 were transfected with GaLV or GaLVΔR and syncytia formation was quantified using the previously implemented method based on cell size distribution (section 3.1.3). Non-transfected cell populations were used as controls.

The microscopical analysis showed that for all the 293T Cas9 complemented cells (mCherry, PiT-1 or PiT-2), the expression of GaLVΔR led to syncytia formation. It was noteworthy that the overexpression of PiT-1 in 293T Cas9 also led to syncytia formation when these cells expressed non-modified GaLV and not only GaLVΔR (**Figure 3.10**).

Regarding the 293T PiT-1 KO cells, the complementation of these cells with PiT-1 led to the formation of syncytia, when they were transfected with GaLVΔR. The complementation of 293T PiT-1 KO with either PiT-2 or mCherry did not lead to syncytia formation when expressing GaLVΔR (**Figure 3.10**), strongly suggesting a cause-effect relation between PiT-1 deletion and the absence of syncytia formation.

Microscopic data results were corroborated with syncytia quantification assay (**Table 3.4**). However, the percentage of events above maximum size in 293T PiT-1 KO cells complemented with PiT-1 and transiently expressing GaLVΔR was expected to be higher. This small increase relatively to GaLV transfected cells might be justified by the fact that syncytia formation in 293T PiT-1 KO complemented with PiT-1 occurred on a much smaller scale than it normally happens in 293T or 293T Cas9 cells.

Table 3. 4 – Syncytia quantification method based on cell size distribution in complemented cell population

Cell line	Complementation	Glycoprotein	Maximum size (µm)[a]	Event above maximum size (%)[b]
293T Cas9	mCherry	Non-transfected	99	-
		GaLV	75	0.0
		GaLVΔR	135	6.0
	PiT-1	Non-transfected	54	-
		GaLV	96	36.1
		GaLVΔR	87	33.3
	PiT-2	Non-transfected	59	-
		GaLV	69	4.1
		GaLVΔR	66	7.0
293T PiT-1 KO	mCherry	Non-transfected	57	-
		GaLV	68	0.2
		GaLVΔR	64	0.2
	PiT-1	Non-transfected	76	-
		GaLV	61	0.0
		GaLVΔR	92	0.3
	PiT-2	Non-transfected	115	-
		GaLV	64	0.0
		GaLVΔR	52	0.0

[a] Maximum event size detected using Cedex HiRes Analyser. [b] Percentage (%) of events with size above the non-transfected maximum.

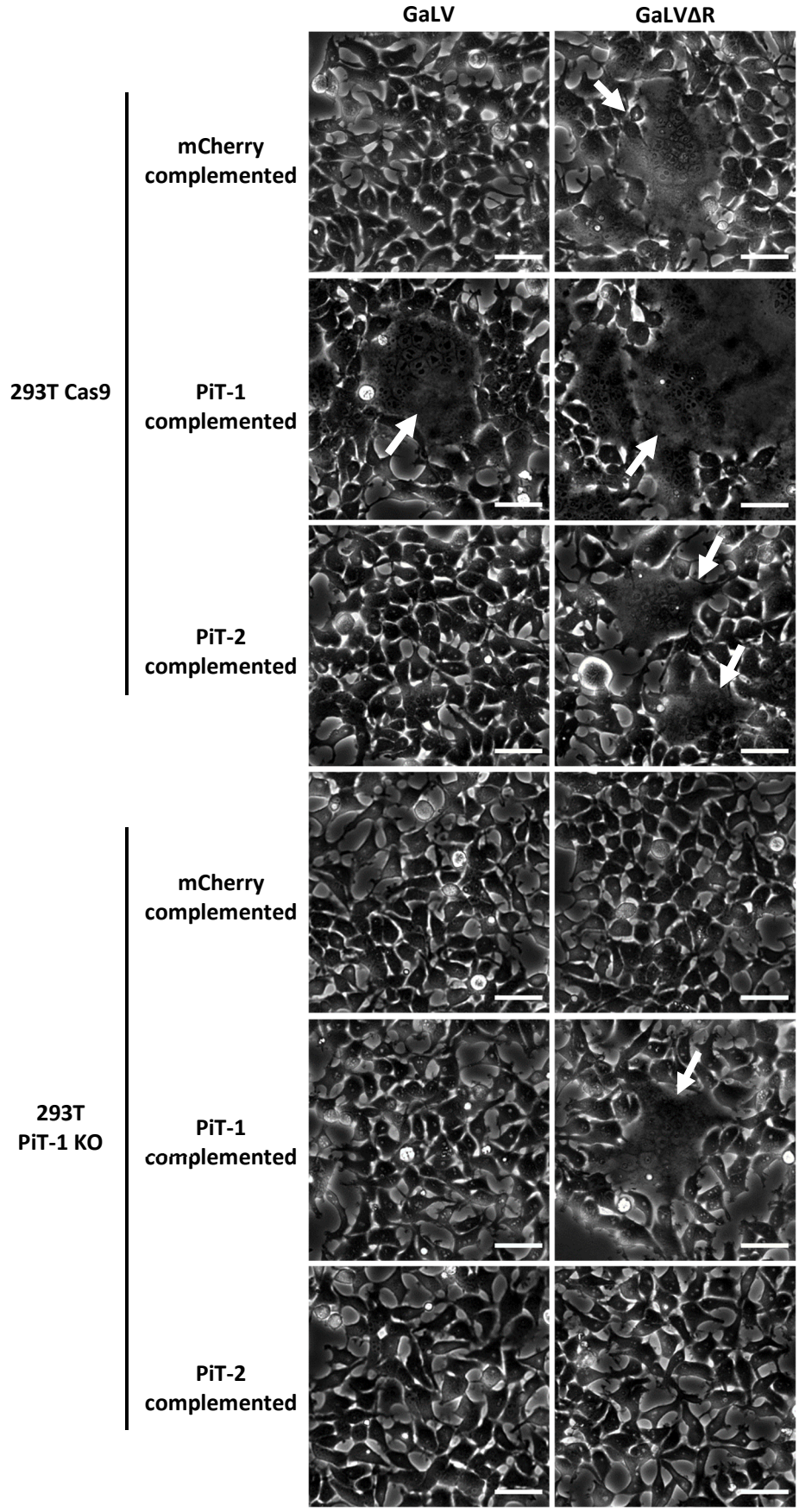

Figure 3. 10 – Syncytia formation in complemented cells. 293T Cas9 and 293T PiT-1 KO cell populations complemented with mCherry, PiT-1 or PiT-2 were transfected with GaLV or GaLVΔR envelope glycoproteins to evaluate syncytia formation. Non-transfected cells were used as negative control (not shown). Images obtained by phase-contrast microscopy. Scale bar: 50 µm White arrows indicate syncytia formation.

3.2. Stable expression of GaLV engineered envelope glycoproteins

3.2.1. New plasmid backbones for stable expression of GaLVs.

We initially used GaLV engineered envelope glycoproteins, for LV pseudotyping, encoded in a *pCMV* backbone plasmid (**Figure 3.11 A**). However, when these constructs were used to establish new stable cell lines, no LV infectious particles titers were obtained although the reason for that outcome was unclear (previous unpublished observations). Therefore, new plasmids encoding these envelope glycoproteins (**Figure 3.11 C**) were created using a plasmid backbone validated for stable expression of LV envelope glycoproteins – *pMonoZeo-4070A* (**Figure 3.11 B**). This plasmid was chosen because it had been successfully used in LentiPro26 cell line [45].

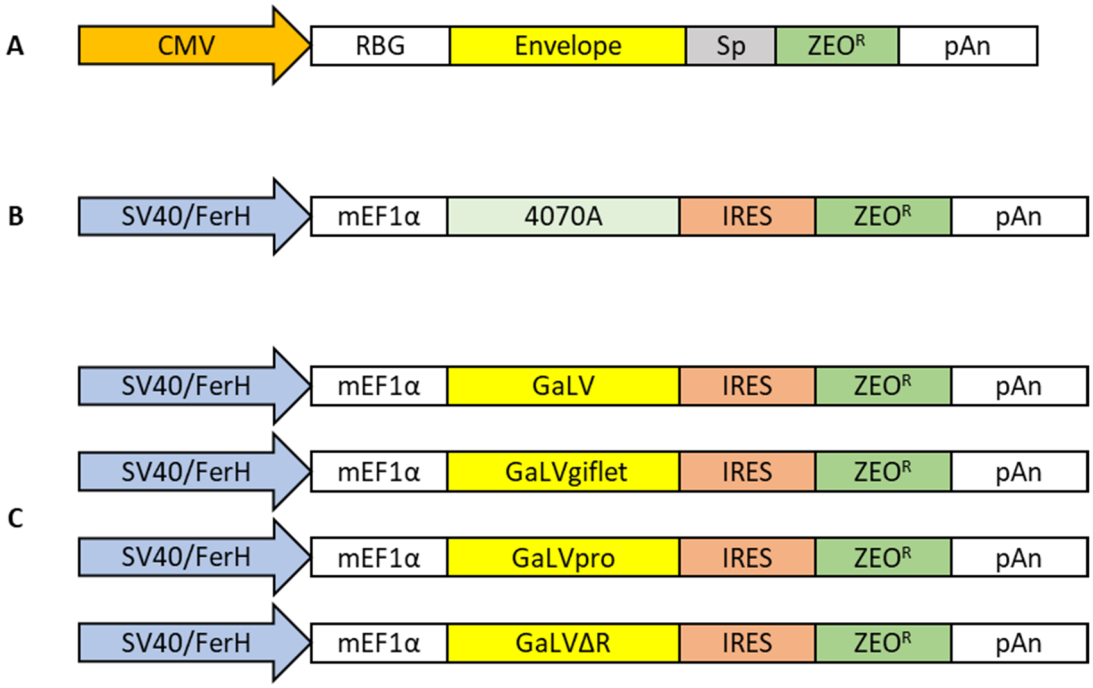

Figure 3. 11 – New envelope glycoprotein plasmids developed in this work. *pCMV*-envelope (A) and *pMonoZeo-4070A* (B) represent the original plasmids (envelope glycoprotein sequence donor and the new plasmid backbone, respectively) used to construct the new plasmids (C) used in envelope glycoprotein stable expression. Main features of each plasmids: CMV- Cytomegalovirus promoter, RBG- rabbit beta-globin intron, Sp- spacer for re-initiation of translation [75,76], ZEO^R- zeocin resistance marker, pAn- polyadenylation signal, 4070A- Murine Leukemia Virus amphotropic envelope glycoprotein, SV40/FerH- SV40 enhancer and a ferritin heavy chain composite protomer, mEF1α- mouse elongation factor 1 alpha gene 5' UTR, IRES- FMDV internal ribosome entry site.

Before proceeding to stable cell selection, the functionality of the new constructs was evaluated in transient LV production. The infectious particles titers obtained with *pCMV* or *pMonoZeo* backbones were similar for both plasmids, independently of the envelope glycoprotein being tested (**Figure 3.12**).

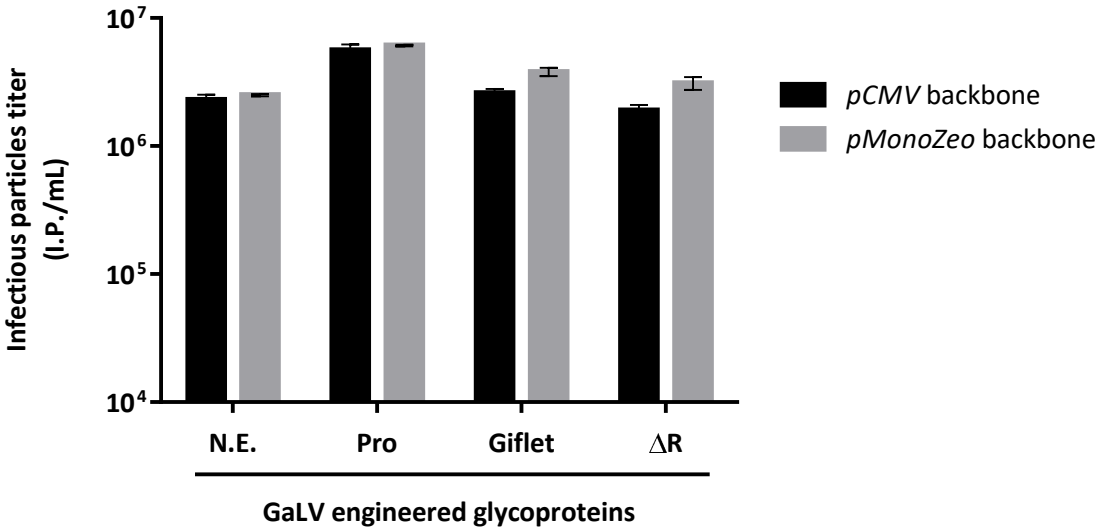

Figure 3. 12 – Titers of lentiviral vectors pseudotyped with GaLV envelope glycoproteins encoded in different plasmid backbones. Infectious particles titers (I.P./mL) of LV vectors pseudotyped with non-engineered GaLV (N.E.) and GaLV engineered envelope glycoproteins encoded in *pCMV* or *pMonoZeo* plasmid backbone, produced in 293T cell line. I.P./mL are shown as average ± standard deviation of two technical replicates.

3.2.2. Establishment of cell populations stably expressing GaLV engineered envelope glycoproteins

293T and 293T PiT-1 KO cell lines were stably transfected with each of the new GaLV envelope glycoproteins expression plasmids, comprising a total of 8 cell populations. Additionally, 293T were also stably transfected with GaLV encoded by the *pCMV* plasmid backbone in an attempt to understand the previous failure to establish a functional stable producer cell line with this plasmid.

The selection of a 293T cell population stably expressing GaLVΔR was not possible due to syncytia formation. However, we were able to select a 293T PiT-1 KO cell population stably expressing this glycoprotein, despite being the last cell population to be selected. Regarding the remaining GaLV engineered envelope glycoproteins, it was possible to select cell populations stably expressing each one of them with both 293T and 293T PiT-1 KO cell lines. Of note, the selection process of 293T PiT-1 KO stably expressing GaLVgiflet or GaLVΔR took an abnormally long period of time when compared to the other cell populations (**Figure 3.13**).

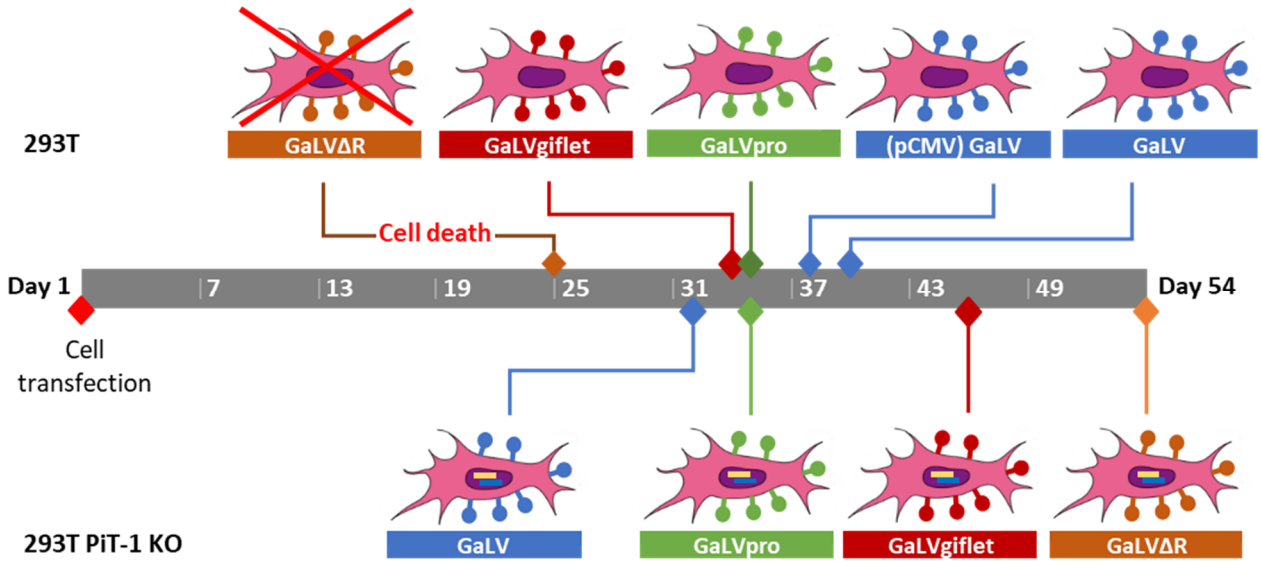

Figure 3. 13 – Cell selection timeline. Timeline of the 293T and 293T PiT-1 KO cell population selection process. The envelope glycoproteins encoded in *pMonoZeo* plasmid are represented in blue, green, red and orange (GaLV, GaLVpro, GaLVgiflet and GaLVΔR, respectively). GaLV encoded in the *pCMV* plasmid is represented in blue as (*pCMV*)GaLV. Red cross indicates cell death.

3.2.3. Quantification of GaLV engineered envelope glycoproteins stable expression

After successfully selecting cell populations, we analysed gene and glycoprotein expression levels through RT-qPCR and live cell surface glycoprotein quantification by immunofluorescence, respectively. PCR amplification efficiency was previously confirmed to be the same for all the envelope glycoproteins (**Figure A.2**, in annexes).

Regarding *pMonoZeo* backbone, the highest mRNA levels were obtained for GaLV, followed by GaLVgiflet and GaLVpro both in 293T and 293T PiT-1 KO cells. Additionally, GaLVΔR achieved mRNA levels similar to those obtained for GaLVpro in 293T PiT-1 KO. Considering the *pCMV* backbone, GaLV mRNA levels were undetectable in 293T stably selected for this construction (**Figure 3.14**).

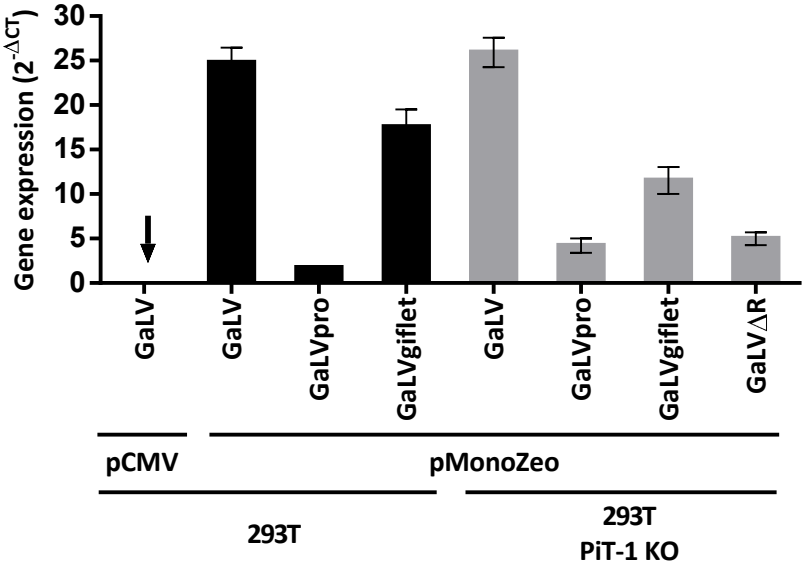

Figure 3. 14 – Gene expression of GaLV engineered envelope glycoproteins in stably selected cells. mRNA levels in 293T and 293T PiT-1 KO cell populations stably expressing GaLV engineered envelope glycoproteins. Gene expression was quantified using the $2^{-\Delta CT}$ method, after normalization to *RPL22* gene (control gene). Gene expression values are shown as average ± standard deviation of two technical replicates. Black arrow indicates the absence of gene expression.

To complement the mRNA levels assessment, we further quantified the expression of envelope glycoprotein expressed at the cellular surface of each population. This quantification was performed by staining with an antibody against the GaLV envelope glycoprotein, targeting a conserved region of the envelope glycoproteins. 293T (without envelope glycoprotein) were used as negative control and 293 FLEX S11 stably expressing GaLV envelope glycoprotein were used as positive control for the staining protocol.

All stably selected populations were considered positive for GaLV envelope glycoprotein expression based on a threshold of more than 80% of positive cells (**Table 3.5**). The exception was the cell population with *pCMV-GaLV10A1*, were no expression was detected.

Table 3. 5 – Percentage of cells expressing GaLV engineered envelope glycoproteins.

Cell line	Plasmid backbone[a]	Envelope glycoprotein	GaLV positive cells (% ± STDev)
293T	-	-	1.79
293 FLEX S11	-	GaLV	98.0 ± 0.1
293T	*pCMV*	GaLV	1.2 ± 0.2
	pMonoZeo	GaLV	98.2 ± 0.1
		GaLVpro	82.2 ± 0.6
		GaLVgiflet	97.5 ± 0.0
293T PiT-1 KO	*pMonoZeo*	GaLV	97.8 ± 0.2
		GaLVpro	94.3 ± 1.6
		GaLVgiflet	94.9 ± 0.8
		GaLVΔR	92.0 ± 0.7

[a]Plasmid backbone encoding the envelope glycoprotein

Concerning envelope glycoprotein expression intensity, GaLV glycoprotein had the highest levels of protein expression in both cell lines, followed by GaLVgiflet and GaLVpro (**Figure 3.15 A**). GaLVΔR had similar

protein expression levels to those observed in 293T PiT-1 KO stably expressing GaLVpro (**Figure 3.15 A**). GaLVgiflet stable expression resulted in two subpopulations with different intensity levels in both 293T and 293T PiT-1 KO, although less visible in the latter (**Figure 3.15 B**).

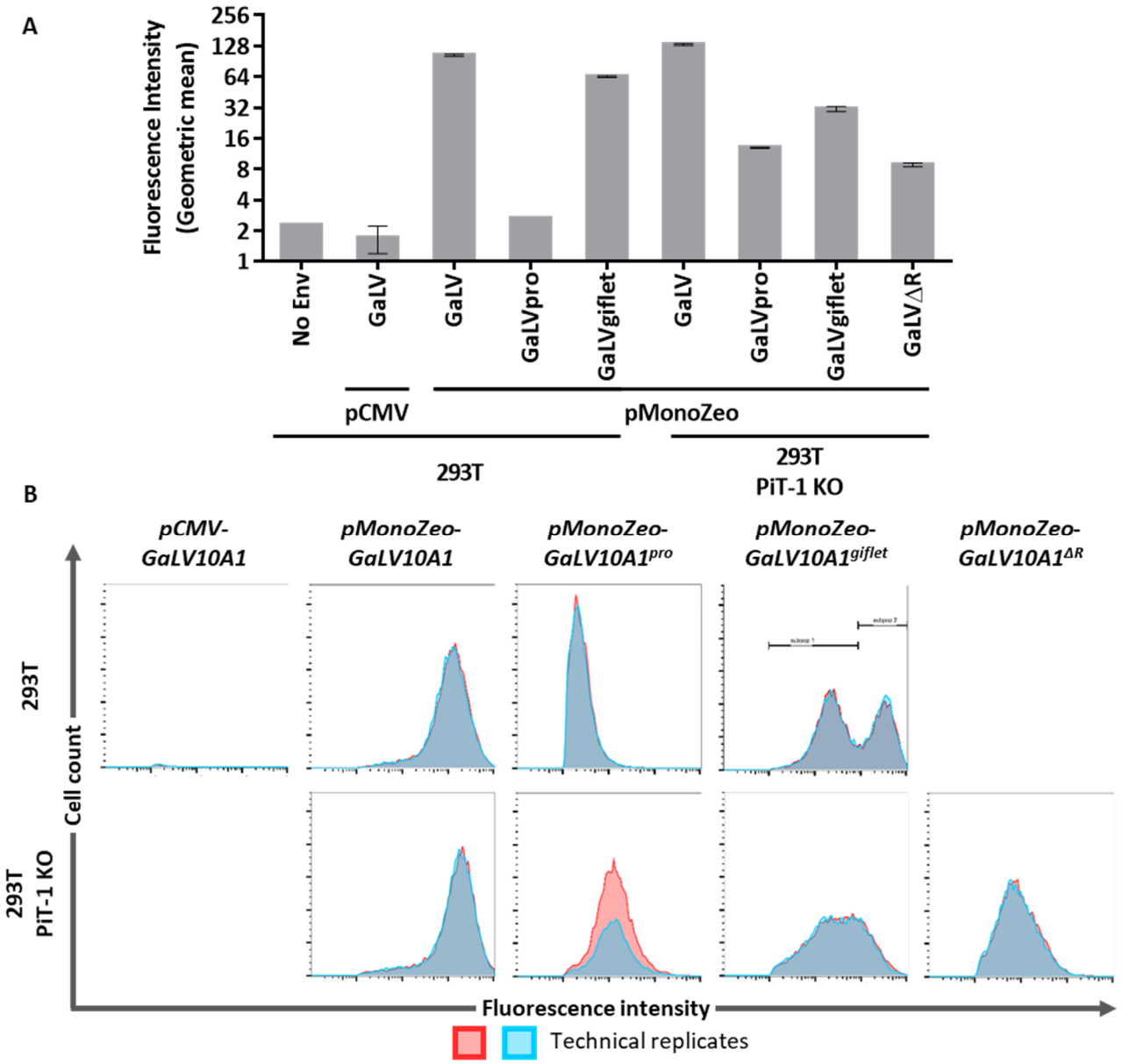

Figure 3. 15 – Cell surface expression of envelope glycoprotein in the several GaLV populations. Quantification of envelope glycoprotein expression at cell surface, by immunofluorescence, in 293T and 293T PiT-1 KO cell populations stably expressing GaLV engineered envelope glycoproteins (encoded in *pCMV* or *pMonoZeo* plasmid backbones). A) Fluorescence intensity (geometric mean) is given as arbitrary units and shown as average ± standard deviation of two technical replicates. B) Red and blue histograms (technical replicates) represent the distribution of fluorescence intensity associated to each cell (only positive cells are shown). Envelope glycoproteins were quantified using an antibody against GaLV glycoprotein as described in materials and methods. Data obtained by flow cytometry and analysed using FlowJo™ software. The same scale was used in every histogram.

After analysing GaLV envelope glycoproteins stable expression levels, we evaluated the relation between the mRNA and glycoprotein expression levels. The results showed that higher mRNA levels translated to higher glycoprotein expression levels (**Figure 3.16**).

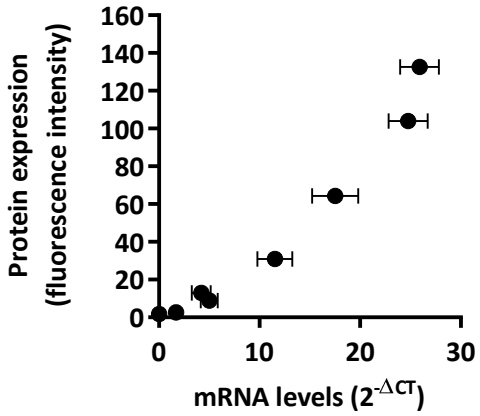

Figure 3. 16 – Relation between mRNA and glycoprotein expression levels on cell surface. mRNA and envelope glycoprotein expression levels from cell populations stably expressing GaLV engineered envelope glycoproteins. Gene expression was quantified using the $2^{-\Delta CT}$ method, after normalization to *RPL22* gene (control gene). Fluorescence intensity (geometric mean), in arbitrary units, was determined by immunofluorescence. Gene expression and fluorescence intensity values are shown as average ± standard deviation of two technical replicates.

3.2.4. Growth studies

The next step in the characterization of our cell populations was to evaluate the impact of expression of GaLV engineered envelope glycoproteins in cell growth.

The growth study showed that 293T stably expressing GaLVpro or GaLVgiflet maintained a growth profile similar to 293T. On the other hand, cell populations expressing either *pCMV-GaLV10A1* or *pMonoZeo-GaLV10A1* experienced a decrease in cell growth (**Table 3.6** and **Figure 3.17**).

Table 3. 6 – Specific cell growth rates of 293T stably expressing GaLV engineered envelope glycoproteins

Cell line	Backbone	Glycoprotein	Specific growth rate (h^{-1})
293T	-	-	0.035±0.002
	pCMV	GaLV	0.029±0.002
	pMonoZeo	GaLV	0.032±0.002
		GaLVpro	0.036±0.001
		GaLVgiflet	0.038±0.001

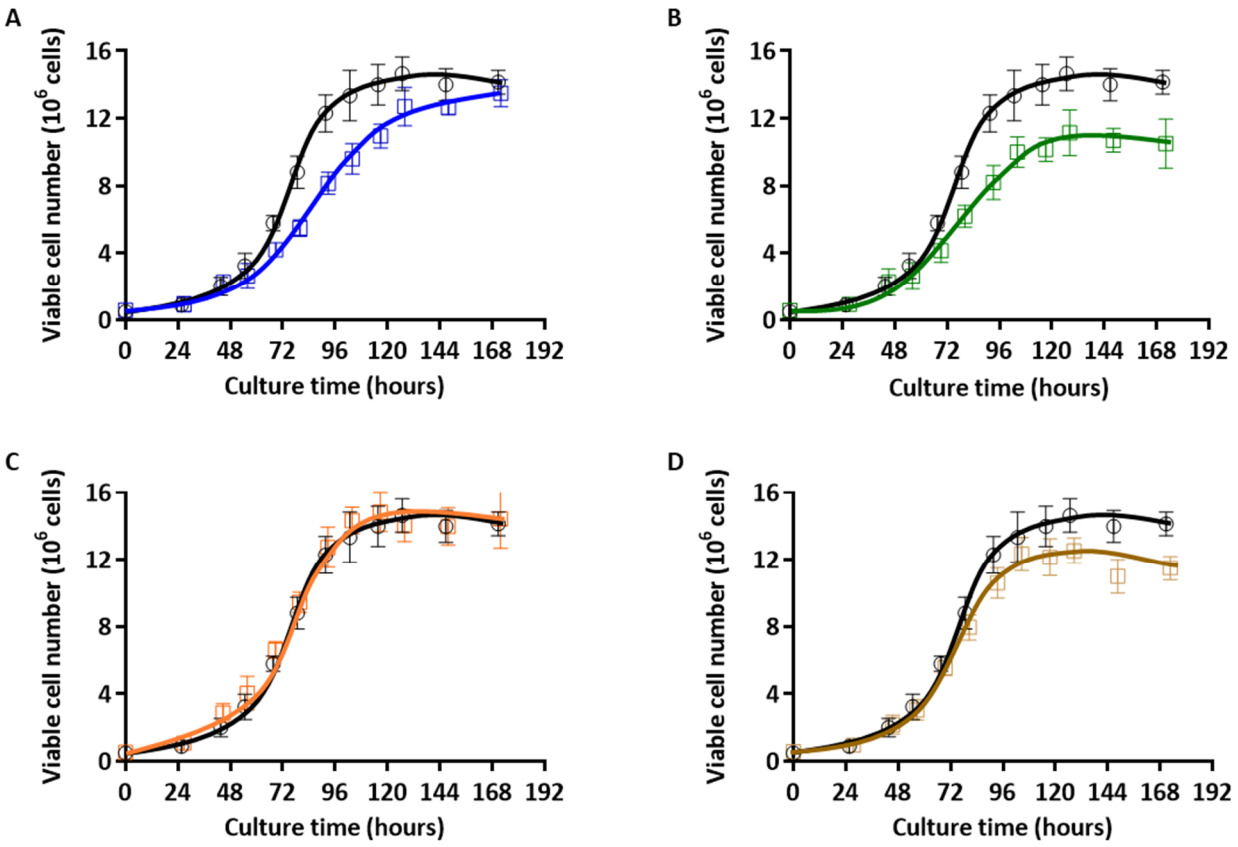

Figure 3. 17 – Growth curves of 293T cells stably expressing GaLV engineered envelope glycoproteins. Values are shown as 10^6 viable cells per t-flask (25 cm^2) and error bars correspond to the standard deviation associated to each cell count on the Cedex HiRes analyser. Blue, green, orange and brown colours represent 293T cell populations stably expressing: A) GaLV encoded in *pCMV* plasmid backbone (□), B) GaLV encoded in *pMonoZeo* plasmid backbone (□), C) GaLVpro encoded in *pMonoZeo* plasmid backbone (□) or D) GaLVgiflet encoded in *pMonoZeo* plasmid backbone (□), respectively. 293T cells were used as growth control (○). Growth curve lines do not have any mathematical significance.

293T PiT-1 KO cells stably expressing GaLVpro or GaLVgiflet, they maintained a similar growth rate relatively to those not expressing envelope glycoproteins (**Table 3.7** and **Figure 3.18 B** and **C**). 293T PiT-1 KO stably expressing GaLV also exhibited a similar growth rate to 293T PiT-1 KO, despite not being able to achieve cell densities as high as 293T PiT-1 KO (**Table 3.7** and **Figure 3.18 A**). However, the cell population stably expressing GaLVΔR glycoprotein experienced a delay in cell growth, which seems to be derived from a longer lag phase (**Table 3.7** and **Figure 3.18 D**).

Table 3. 7 – Specific growth rates of 293T PiT-1 KO stably expressing GaLV engineered envelope glycoprotein

Cell line	Backbone	Glycoprotein	Specific growth rate (h^{-1})
293T PiT-1 KO	-	-	0.030±0.001
	pMonoZeo	GaLV	0.029±0.001
		GaLVpro	0.028±0.001
		GaLVgiflet	0.029±0.001
		GaLVΔR	0.027±0.001

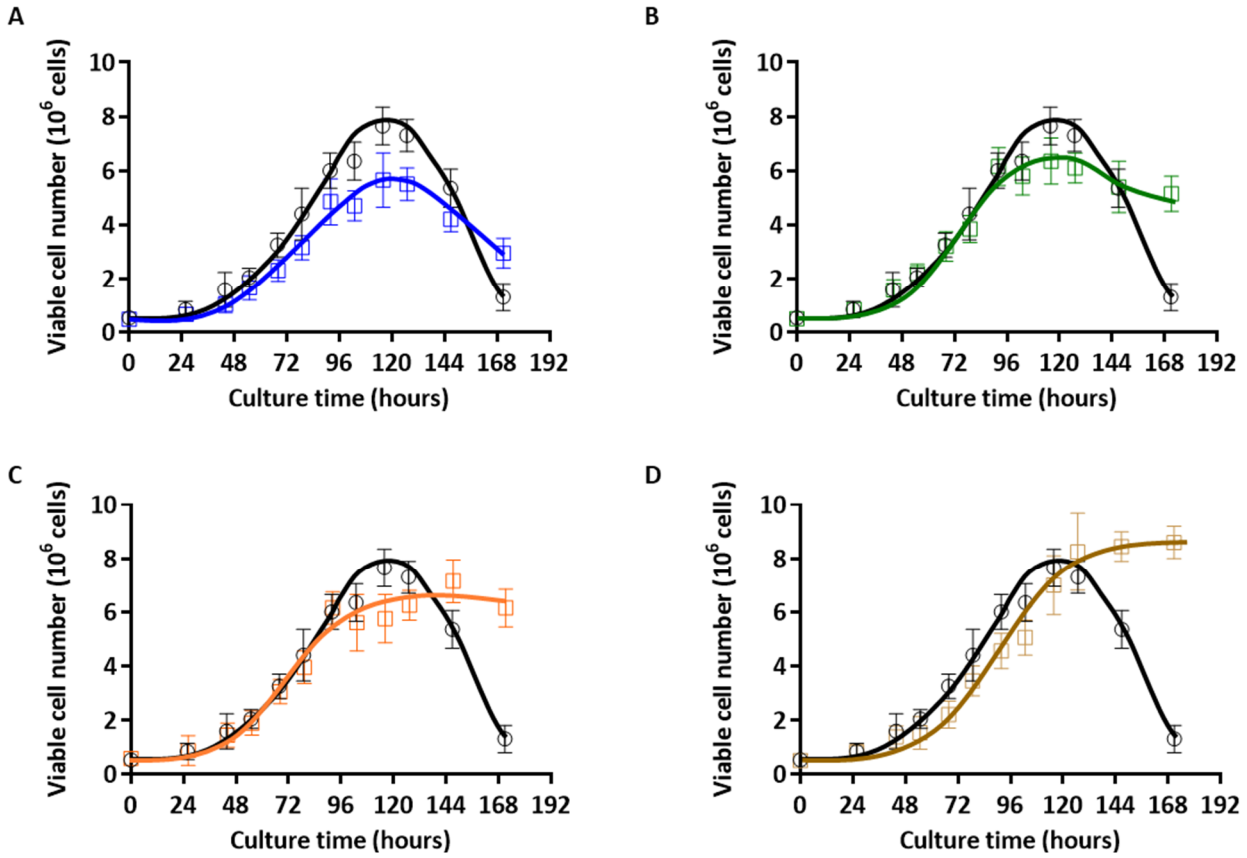

Figure 3. 18 – Growth curves of 293T PiT-1 KO cells stably expressing GaLV engineered envelope glycoproteins. Values are shown as 10^6 viable cells per t-flask (25 cm^2) and error bars correspond to the standard deviation associated to each cell count on the Cedex HiRes analyser. Blue, green, orange and brown colours represent 293T PiT-1 KO cell populations stably expressing: A) GaLV (□), B) GaLVpro (□), C) GaLVgiflet (□) or D) GaLVΔR (□), encoded in the *pMonoZeo* backbone. 293T PiT-1 KO cells were used as growth control (○). Growth curve lines do not have any mathematical significance.

3.3. Lentiviral vector production in cell populations stably expressing GaLV envelope glycoproteins

After characterizing the growth of cells constitutively expressing GaLV engineered envelope glycoproteins and confirmed the expression of each protein, we evaluated the potential of these cells for LV production. This assessment was done by performing a semi-stable LV production where each cell population was transiently transfected with the remaining components needed for a LV production (packaging and transgene plasmids), using a stuffer plasmid instead of the envelope glycoprotein, to maintain the standard plasmid DNA amounts and proportions. A parallel production was also performed – supplemented semi-stable LV production - where each cell population was transfected with all the plasmid components, including the envelope glycoprotein plasmid (**Figure 3.19**). 293T transfected with VSV-G envelope glycoprotein was used as LV production control (data not shown). A standard transient LV production with cells not expressing any of the envelope glycoproteins was performed for comparison (**Figure 3.19**).

The results showed that, independently of the producer cell population, infectious particles titers from the semi-stable production were near or below the detection limit associated to the flow cytometry titration method (4.0 x 10^4 I.P./mL) (**Figure 3.19**). When supplementing with more envelope glycoprotein by

transient transfection, only 293T stably expressing GaLVpro and 293T PiT-1 KO stably expressing GaLVΔR showed to increase their LV productivity to approximately 10^6 I.P./mL (**Figure 3.20**). The remaining cells generated a small increase in LV titers (in the order of 10^5 I.P./mL) in comparison to the non-supplemented semi-stable production (**Figure 3.19**). Comparatively to the transient production, only 293T stably expressing GaLVpro and 293T PiT-1 KO stably expressing GaLVΔR in the supplemented semi-stable production setting were able to achieve LV titers similar to those obtained in a standard transient LV production. (**Figure 3.19**).

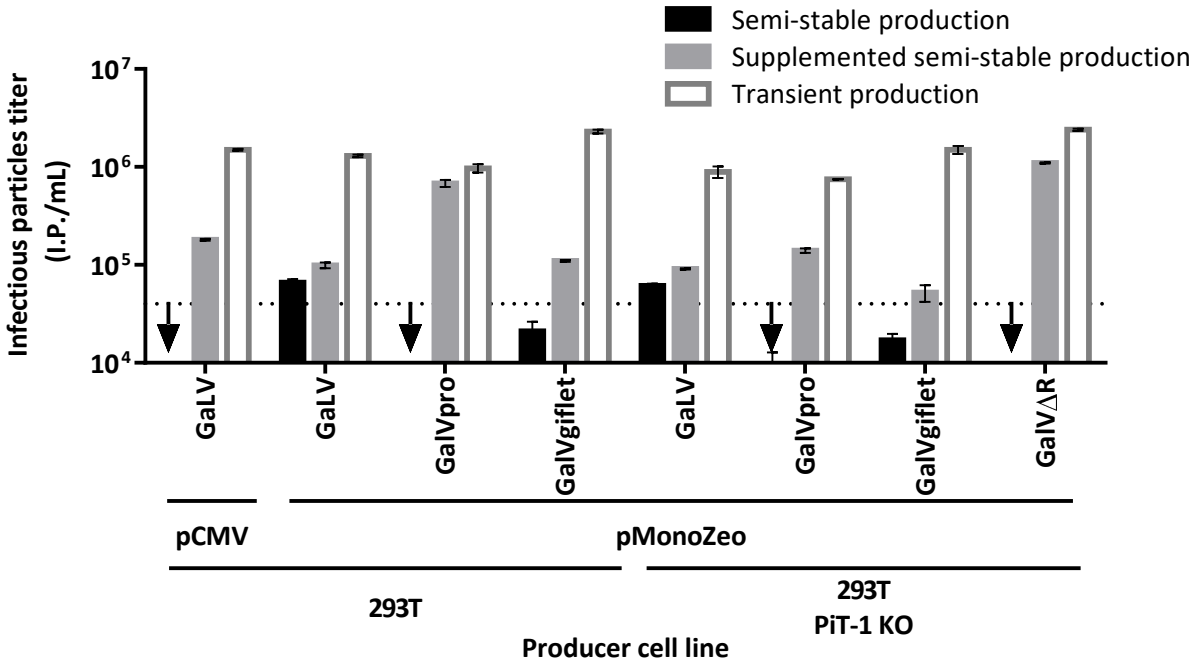

Figure 3. 19 – Impact of envelope glycoproteins stable expression in LV productivity. LV produced with cell populations stably expressing GaLV engineered envelope glycoproteins (encoded in *pCMV* or *pMonoZeo* plasmid) in a semi-stable or in a supplemented semi-stable LV production setting. A transient production using each envelope glycoprotein, in 293T and 293T PiT-1 KO not expressing any envelope glycoprotein, was used for comparison. Infectious particles titers (I.P./mL) are shown as average ± standard deviation of two technical replicates. Detection limit of 4.0 x 10^4 I.P./mL associated to the flow cytometry titration method is indicated by a dotted line. Black arrows indicate the absence of infectious particles titers.

Since the LV titers from the semi-stable productions were much lower than those usually obtained in a transient LV production, we compared the transfection efficiencies from the semi-stable and supplemented semi-stable production with those from the transient production. They were plotted against the LV titers to evaluate if there was a relation between LV titers and transfection efficiencies (**Figure 3.20**).

Transfection efficiencies from the semi-stable and supplemented semi-stable production were generally lower than those obtained in a standard transient production (**Figure 3.20**). However, no relation was found between reduced LV titers and lower transfection efficiencies (**Figure 3.20**).

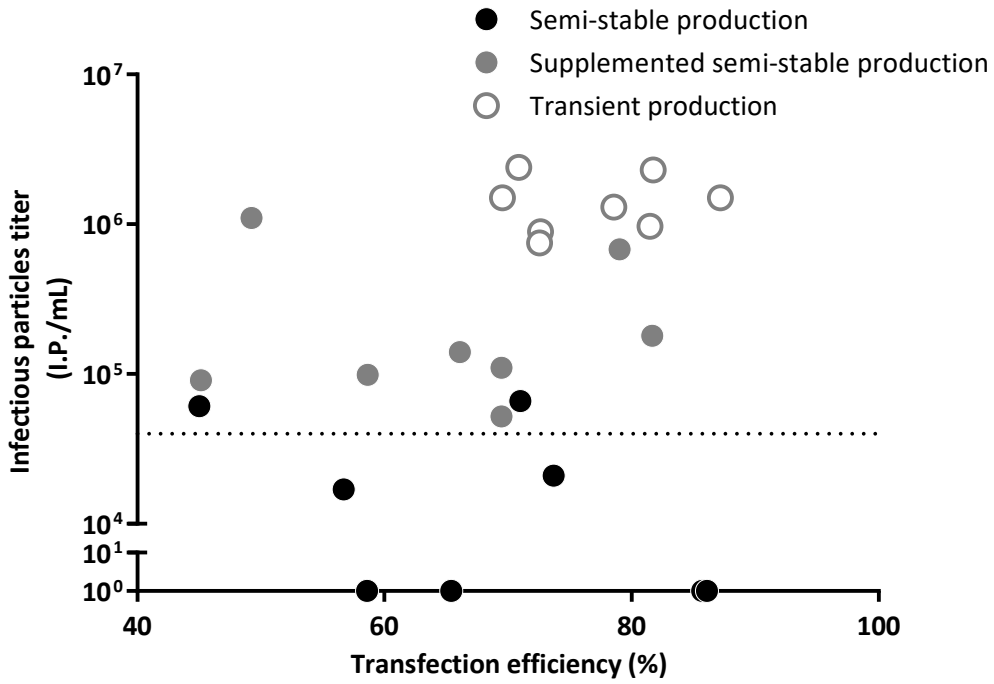

Figure 3. 20 – Transfection efficiencies vs LV titers. LV titers and transfection efficiencies from the semi-stable, supplemented semi-stable and transient LV production. Transfection efficiencies are shown in percentage (%). Infectious particles titers (I.P./mL) are shown as average ± standard deviation of two technical replicates. Detection limit of 4.0 x 10^4 I.P./mL associated to the flow cytometry titration method is indicated by a dotted line. LV titers bellow 10^4 I.P./mL were considered 1 I.P./mL.

Transfection efficiencies from both the semi-stable and the supplemented semi-stable LV production were then plotted against envelope glycoprotein mRNA levels. The results showed no relation between transfection efficiencies and *GaLV* mRNA levels (**Figure 3.21**). However, the first points corresponding to almost no *GaLV* gene expression, achieved the highest transfection efficiencies. This suggest that there might exist a *GaLV* expression threshold around 2 or 3 ($2^{-\Delta CT}$) from which transfection efficiency starts to decrease.

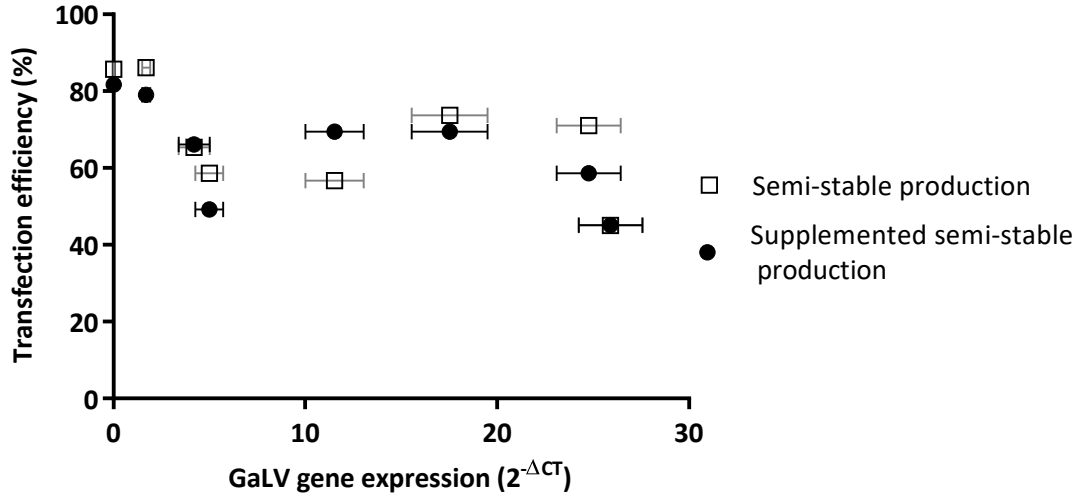

Figure 3. 21 – Transfection efficiencies vs GaLV mRNA levels. Transfection efficiencies from the semi-stable and supplemented semi-stable LV productions plotted against the mRNA levels of GaLV engineered envelope glycoproteins. Transfection efficiencies are shown in percentage (%). Gene expression was quantified using the $2^{-\Delta CT}$ method, after normalization to *RPL22* gene (control gene). Gene expression values are shown as average ± standard deviation of two technical replicates.

Since the LV titers from the semi-stable production were much lower than those from the standard transient production, we compared the envelope glycoprotein mRNA levels in the transient production to those obtained in stable expression (in **Figure 3.14**). The results showed that only cells stably expressing GaLVpro or GaLVΔR had substantial differences in terms of envelope glycoprotein mRNA levels, presenting lower mRNA levels in stable than in transient expression (**Figure 3.22**).

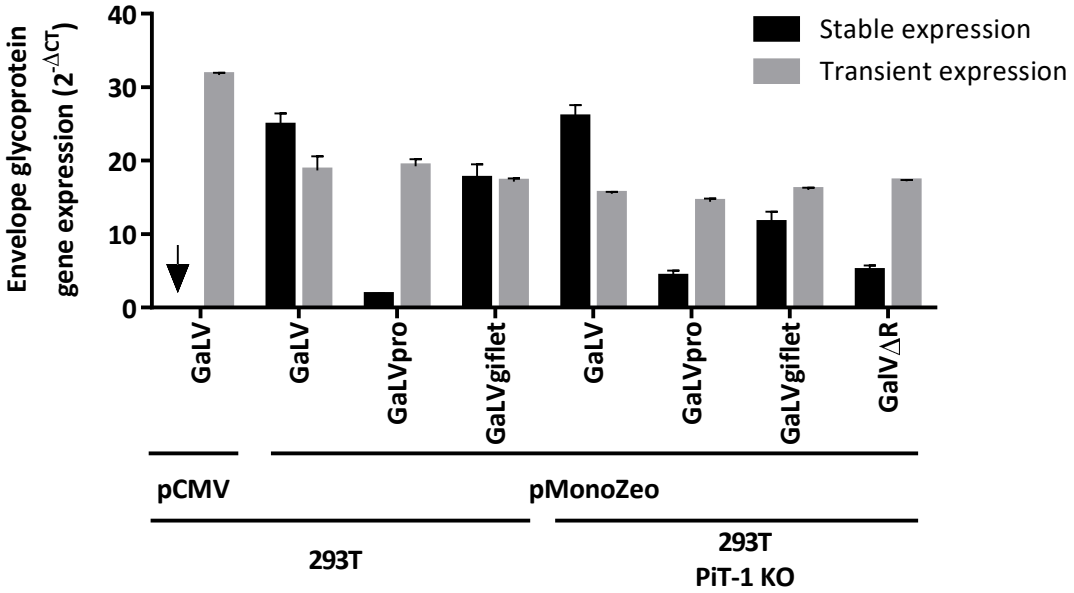

Figure 3. 22 – Envelope glycoprotein mRNA levels in transient and stable expression. Envelope glycoprotein mRNA levels in 293T and 293T PiT-1 KO cell populations stably expressing GaLV engineered envelope glycoproteins (encoded in *pCMV* or *pMonoZeo* plasmid backbone) and envelope glycoprotein mRNA levels in a transient LV production in 293T and 293T PiT-1 KO cell lines (not stably expressing any envelope glycoprotein). Gene expression was quantified using the $2^{-\Delta CT}$ method, after normalization to *RPL22* gene (control gene). Gene expression values are shown as average ± standard deviation of two technical replicates. Black arrow indicates the absence of mRNA levels. In the absence of biological replicates a 2-fold variance is considered as relevant differences, with no statistical significance claimed.

4. Discussion and Conclusions

The potential of gene therapy to treat a broad range of diseases, ranging from cancer to monogenic diseases, makes it a powerful approach to address medical needs that are currently unmet by conventional medicine [77,78]. In the past years, LV have been the viral vectors presenting the highest growth in gene therapy clinical trials [2]. This is mainly due to their large genetic payload (up to 9kb), the ability to transduce both dividing and non-dividing cells, permanently integrating into the target cell genome allowing life-long expression of the transgene and increased safety when compared to *Gammaretrovirus* [9–11,79]. This makes LV particularly interesting for gene therapy applications that require the transduction of non-proliferating cells and long-term expression of the transgene.

To consolidate clinical-to-market transition, the establishment of robust and scalable LV production systems becomes imperative. In this context, constitutive LV producer cell lines will ensure a cost-effective and more standardized alternative for large-scale LV production comparatively to transient production [34,35]. However, the development of such cell lines has been challenged by the cytotoxicity associated to the components required for LV production, namely the VSV-G envelope glycoprotein, currently used for LV pseudotyping [29,35]. To circumvent this problem, non-cytotoxic envelope glycoproteins, such as GaLV, have been used to develop new stable producer cell lines [44].

The main goal of this thesis was to evaluate the potential of the high-titer GaLVΔR envelope glycoprotein for stable expression, in order to enable its use in constitutive LV producer cells. Due to its intrinsic capacity to induce the formation of syncytia in 293T cells [55], we used the 293T PiT-1 KO cell line as our starting cells. This cell line supports GaLVΔR expression due to CRISPR/Cas9 knock-out of the GaLV cell receptor: PiT-1. Based on these cells, and aiming to study the potential of GaLVΔR in stable expression, this project was divided in three lines of work: i) characterization of 293T PiT-1 KO phenotype; ii) stable expression of GaLV engineered envelope glycoproteins and iii) evaluation of LV production potential. Throughout this work, 293T and 293T Cas9 (stably expressing the Cas9 endonuclease) cell lines were used as controls and terms of comparison to 293T PiT-1 KO.

The deletion of PiT-1 led to a decrease in both cell growth rate and maximum cell density (**Table 3.1 and Figure 3.2 A**). Since PiT-1 is an inorganic phosphate transporter, we hypothesized that the decrease in cell growth could derive from alterations in the uptake of inorganic phosphate, essential for key cellular functions, such as lipid and nucleic acid synthesis or signal transduction [61]. If this hypothesis was true, the complementation of 293T PiT-1 KO with PiT1 or another phosphate transporter (such as PiT-2) should improve cell growth. Indeed, when 293T PiT-1 KO were complemented with any of these two phosphate transporters, we were able to rescue 293T PiT-1 KO growth to the original rate of 293T cells (**Table 3.3 and Figure 3.9 A**). This supports the hypothesis that the reduced cell growth was, in fact, caused by alterations in

inorganic phosphate uptake. Further impact of PiT-1 depletion in cell proliferation has been described by Beck *et al.* [80].

293T PiT-1 KO experienced an early drop in cell viability comparatively to 293T (**Figure 3.2 B**). The fact that this decrease was also observed in 293T Cas9 cells, suggested that the drop in cell viability was not linked to PiT-1 KO but related to Cas9 expression in both cell lines. Constitutive expression of Cas9 seems to be inducing some level of cytotoxicity most likely due to the well-known off-target effects in non-specific DNA sequences [81,82]. These results point to the need to use an alternative strategy when using Cas9, namely by transient expression of this endonuclease.

Despite the decrease on 293T PiT-1 KO cell growth, no significant changes were observed in LV infectious particles titers, in any of the tested envelope glycoproteins (**Figure 3.3**). This excludes any role of PiT-1 in LV replication and assembly and corroborates the use of the PiT-1 KO strategy as a good methodology for the development of LV producer cell lines, constitutively expressing GaLVΔR.

293T PiT-1 KO complementation studies served not only to rescue cell growth but to probe a potential cause-effect relation between PiT-1 KO and the resistance to syncytia formation. Additionally, the establishment of PiT-2 complemented cells served to evaluate if syncytia formation induced by GaLVΔR was specific to PiT-1 expression and not to other proteins with a similar cellular function. The quantification of *PiT-1* and *PiT-2* gene expression confirmed the success of the complementation, achieving expression levels superior to those observed in non-complemented cells (**Figure 3.6**). However, this could not be corroborated at the protein level (**Figure 3.7**), due to what seemed to be the result of the use of not suitable antibodies in the western blot. Hence, a new set of antibodies should be tested in a future approach. The detection of PiT-1 and PiT-2 expression by immunofluorescence also provides an alternative approach for protein quantification.

To gain quantitative insights on the phenotype of syncytia formation and not to solely rely on subjective microscopic analysis (**Figure 3.4**), we developed a method for syncytia quantification. This method is based on an image-based cell analyser (Cedex HiRes Analyser) combined with statistical analysis. This method successfully provided quantitative evidences on the resistance to syncytia formation of 293T PiT-1 KO when expressing GaLVΔR (**Table 3.2** and **Figure 3.5**). This method was also used to evaluate syncytia formation in cell populations of 293T PiT-1 KO complemented (**Table 3.4**). The complementation of 293T PiT-1 KO cells with PiT-1 restored the syncytia formation phenotype, strongly supporting the cause-effect relation between the PiT-1 KO and the resistance to syncytia formation in 293T PiT-1 KO. Additionally, the absence of syncytia in PiT-2 complemented cells corroborated that syncytia formation with GaLVΔR expression is specific to the presence of PiT-1 and cannot be induced by the expression of other proteins with similar functions. Remarkably, the overexpression of PiT-1 in 293T Cas9 led to the formation of syncytia simply transfected

with non-modified GaLV (**Figure 3.10** and **Table 3.4**), suggesting that either GaLV retains some fusogenic activity without proteolytic processing or that it can be processed to a lower extent by cellular proteases.

A second line of work of this project was to establish new cell populations stably expressing a set of GaLV engineered envelope glycoproteins: GaLVpro, GaLVgiflet and GaLVΔR. This had already been tested in our laboratory, but the resulting cell populations were unable to produce infectious LV particles, although the underlying reasons were unclear. We hypothesized that, despite their functionality in transient expression, the plasmid encoding these envelope glycoproteins (*pCMV* backbone, **Figure 3.11 A**) might not be functional in stable expression. To work around this problem, we designed new LV pseudotyping plasmids using *pMonoZeo* backbone (**Figure 3.11 B**). This backbone had already proved functional in stable expression since it was used to establish another stable LV producer cell line, LentiPro26 [45]. The construction of these new plasmids and the validation of their functionality in transient expression (**Figure 3.12**) was followed by the selection of stable cell populations constitutively expressing the GaLV engineered envelope glycoproteins. Selection of a cell population stably expressing GaLVΔR construct was not possible in line with the cytotoxicity of syncytia formation (**Figure 3.13**). But, we were able to stably express this construct using 293T PiT-1 KO cells (**Figure 3.13**). This was one of the most significant results of this thesis since it corroborates the PiT-1 KO strategy as the path to create constitutive producer cell lines with GalVΔR. Noteworthy was the increased time for selection of 293T PiT-1 KO cells expressing GaLVgiflet or GalVΔR (**Figure 3.13**) suggesting that the expression of these envelopes might also be associated to some cytotoxicity.

Following stable selection of GaLV (and its derivates) expressing cells we assessed their expression levels. The analysis of *GaLV* mRNA levels, encoded in *pCMV*, confirmed our hypothesis that *pCMV* backbone plasmid is not functional in stable expression (**Figure 3.14**). On the other hand, GaLV encoded in *pMonoZeo* plasmid backbone was successfully expressed in stable, strongly suggesting that the absence of expression with *pCMV* backbone was related only to the plasmid design (**Figure 3.14**). This also answers the question of why previous studies to establish stable producer cell lines with this backbone failed. The reason for *pCMV* being unable to express GaLV in stable expression is unknown. We hypothesize that a selection bias is the cause for this output. In *pCMV* backbone, the zeocin resistance marker expression is linked to the expression of GaLV in a bicistronic cassette. Since we were able to select this cell population under antibiotic pressure, we know that this cassette is being transcribed, although, its mRNA expression levels were undetected by RT-qPCR. The expression of zeocin resistance marker is associated to GaLV expression using a spacer as mechanism of re-initiation of translation. This mechanism pushes the selection of cells with very high levels of protein expression upstream the spacer. On the other hand, GaLV expression seems to induce some level of cytotoxicity. Finally, the entire transcript is driven by a CMV promoter which is known to be prone to long-term silencing in stable expression [83,84]. Therefore, considering the apparent glycoprotein cytotoxicity associated to very high levels of GaLV expression, we hypothesize that we were only able to select cells with very low levels of cassette expression. In contrast to GaLV, which is a structural protein, low expression levels

of the selection marker are usually sufficient to confer resistance. To test this hypothesis, in future work we will repeat the quantification of mRNA levels from these expression cassettes using a different set of primers, this time targeting the zeocin resistance marker gene, in both plasmid backbones.

Relatively to *pMonoZeo* encoded glycoproteins, the pattern of *GaLV*, *GaLVpro* and *GaLVgiflet* mRNA levels was the same in both 293T and 293T PiT-1 KO cell lines (**Figure 3.14**). This suggests that PiT-1 deletion did not affect 293T PiT-1 KO ability to express these glycoproteins. Additionally, similar levels of *GaLVpro* and *GaLVΔR* mRNA expression suggest that ΔR mutation does not impair GaLV expression, at least at the mRNA level. PCR data was fully corroborated by the quantification of cell surface expression of GaLV engineered envelope glycoproteins in live cells (**Table 3.5** and **Figure 3.15**).

To further characterize these populations, we evaluated their cell growth. For 293T derived cells, GaLVpro and GaLVgiflet populations maintained a similar growth pattern, while GaLV cell populations (encoded in either *pCMV* or *pMonoZeo* backbone) experienced a decrease in cell growth comparatively to 293T cells (**Table 3.6** and **Figure 3.17**). Assuming that our hypothesis about the selection bias is correct, the decrease in cell growth of cells expressing GaLV encoded in *pCMV* backbone may be attributed to the fact that we might have selected cells with lower growth, during the selection process (**Table 3.6** and **Figure 3.17 A**). Relatively to GaLV encoded in *pMonoZeo* backbone, the decrease in cell growth might be a consequence of high expression levels of this glycoprotein, considering the apparent cytotoxicity associated with GaLV (**Table 3.6** and **Figure 3.17 B**). For 293T PiT-1 KO cells, the expression of GaLVΔR was the only to induce a delay in cell growth. Together with the fact that this cell population was the last to be selected this suggest that GaLVΔR stable expression still retains some level of cytotoxicity (**Table 3.7** and **Figure 3.18**). It is difficult however to discriminate the origin of this toxicity or associate it to any fusogenic activity of GaLVΔR because even non-fusogenic GaLV seemed to reduce cell growth.

We finally analysed the newly established cell populations stably expressing GaLV for their potential for LV production. In a semi-stable setting, none of the established cell populations were able to produce high titers of infectious LVs (**Figure 3.19**). Additionally, the supplementation of each cell population with more envelope glycoprotein could not restore LV productivity with the exception of 293T GaLVpro and 293T PiT-1 KO GaLVΔR (**Figure 3.19**). This suggests that reduced LV titers are not due to insufficient glycoprotein expression since not even the complementation of envelope glycoprotein was able to rescue LV productivity. This hypothesis was further corroborated by the comparison of the envelope glycoprotein mRNA levels in stable or transient expression (**Figure 3.22**). In fact, data seems to point in the opposite direction. In general, every cell line showed a decrease in transfection efficiency when compared to a standard transient production (**Figure 3.20**). We hypothesize that they might be less permissive to be transfected again for example due to high expression levels of GaLV on the cell surface. This hypothesis holds considering a relation between transfection efficiency, LV titers and glycoprotein mRNA levels (**Figure 3.20** and **Figure 3.21**). Although a correlation is not present, a threshold of gene expression of 2 or 3 ($2^{-\Delta CT}$) might exist, above which

transfection might be compromised (**Figure 3.21**)**.** To evaluate if the reduced transfection efficiencies represent a problem for efficient LV productivity, we can evaluate the levels of mRNA expression from the other components from the LV packaging system and compared them to a standard transient production.

Regardless that this hypothesis is valid, the implications are of low relevance for this project since the ultimate goal is to have functional expression in cells stably expressing all vector components. Hence, in the follow up of this work, we will apply the envelope glycoprotein encoding plasmids herein developed in another cell substrate. These cells already constitutively express all the other components of the LV packaging system with the exception of the envelope glycoprotein. We will not be able to select cells stably expressing GaLVΔR, since these cells express the PiT-1 protein, however we expect to select cells constitutively expressing GaLVpro or GaLVgiflet envelope glycoproteins that also yield higher LV titers comparatively to GaLV [55]. PiT-1 KO strategy can be implemented for these cells based on what we learned in this work, namely by using Cas9 but in transient expression.

In conclusion, we constructed new GaLV envelope glycoprotein encoding plasmids that are fully functional in stable expression. Additionally, we developed an analytical method to quantify syncytia formation based on cell size distribution, which is more robust and less subjective than the pre-existing method based on cell microscopic analysis. This method gave us quantitative evidences for a cause-effect relation between the deletion of PiT-1 and the resistance of 293T PiT-1 KO to syncytia formation. Furthermore, we showed that the reduced cell growth from 293T PiT-1 KO could be restored by PiT-2 complementation. More importantly, we demonstrated that GaLVΔR stable expression is possible. This work serves as proof-of-concept for the envelope glycoprotein cell receptor KO strategy as a valid approach to stably express envelope glycoproteins with fusogenicity-derived cytotoxicity. This thesis unfolds new possibilities and contributes for improved means for the production of LVs for cell and gene therapy.

5. Bibliography

1. Wirth T, Parker N, Ylä-Herttuala S. History of gene therapy. Gene. 2013 Aug 10;525(2):162–9.

2. Edelstein M. Gene Therapy Clinical Trials Worldwide [Internet]. [cited 2019 Sep 13]. Available from: http://www.abedia.com/wiley/index.html

3. Mountain A. Gene therapy: the first decade. Trends Biotechnol. 2000 Mar;18(3):119–28.

4. Rosenberg SA, Aebersold P, Cornetta K, Kasid A, Morgan RA, Moen R, Karson EM, Lotze MT, Yang JC, Topalian SL, Merino MJ, Culver K, Miller AD, Blaese RM, Anderson WF. Gene Transfer into Humans — Immunotherapy of Patients with Advanced Melanoma, Using Tumor-Infiltrating Lymphocytes Modified by Retroviral Gene Transduction. N Engl J Med. 1990 Aug 30;323(9):570–8.

5. Gene Therapy Market Size | Global Industry Growth Report, 2019-2026 [Internet]. [cited 2019 Sep 23]. Available from: https://www.grandviewresearch.com/industry-analysis/gene-therapy-market

6. Gene Therapy Market Size Worth $5.55 Billion By 2026 | CAGR: 33.9% [Internet]. [cited 2019 Sep 23]. Available from: https://www.grandviewresearch.com/press-release/global-gene-therapy-market

7. Crystal RG. In vivo and ex vivo gene therapy strategies to treat tumors using adenovirus gene transfer vectors. Cancer Chemother Pharmacol. 1999 May 12;43(7):S90–9.

8. Nayerossadat N, Ali P, Maedeh T. Viral and nonviral delivery systems for gene delivery. Adv Biomed Res. 2012;1(1):27.

9. Coroadinha AS, Gama-Norton L, Amaral AI, Hauser H, Alves PM, Cruz PE. Production of retroviral vectors: review. Curr Gene Ther. 2010 Dec;10(6):456–73.

10. Naldini L, Blomer U, Gallay P, Ory D, Mulligan R, Gage FH, Verma IM, Trono D. In Vivo Gene Delivery and Stable Transduction of Nondividing Cells by a Lentiviral Vector. Science (80-). 1996 Apr 12;272(5259):263–7.

11. De Palma M. Promoter trapping reveals significant differences in integration site selection between MLV and HIV vectors in primary hematopoietic cells. Blood. 2005 Mar 15;105(6):2307–15.

12. Beard BC, Dickerson D, Beebe K, Gooch C, Fletcher J, Okbinoglu T, Miller DG, Jacobs MA, Kaul R, Kiem H-P, Trobridge GD. Comparison of HIV-derived Lentiviral and MLV-based Gammaretroviral Vector Integration Sites in Primate Repopulating Cells. Mol Ther. 2007 Jul 1;15(7):1356–65.

13. Seimetz D, Heller K, Richter J. Approval of First CAR-Ts: Have we Solved all Hurdles for ATMPs? Cell Med. 2019 Jan 22;11:1–16.

14. International Committee on Taxonomy of Viruses (ICTV) [Internet]. [cited 2019 Oct 13]. Available from: https://talk.ictvonline.org/taxonomy/

15. Campbell RSF, Robinson WF. The comparative pathology of the lentiviruses. J Comp Pathol. 1998 Nov 1;119(4):333–95.

16. Fauci A, Desrosiers R. Pathogenesis of HIV and SIV. In: Coffin J, Hughes S, Varmus H, editors. Retroviruses. Cold Spring Harbor (NY): Cold Spring Harbor Laboratory Press; 1997.

17. Barre-Sinoussi F, Chermann J, Rey F, Nugeyre M, Chamaret S, Gruest J, Dauguet C, Axler-Blin C, Vezinet-Brun F, Rouzioux C, Rozenbaum W, Montagnier L. Isolation of a T-lymphotropic retrovirus from a patient at risk for acquired immune deficiency syndrome (AIDS). Science (80-). 1983 May 20;220(4599):868–71.

18. Gallo R, Sarin P, Gelmann E, Robert-Guroff M, Richardson E, Kalyanaraman V, Mann D, Sidhu G, Stahl R, Zolla-Pazner S, Leibowitch J, Popovic M. Isolation of human T-cell leukemia virus in acquired immune deficiency syndrome (AIDS). Science (80-). 1983 May 20;220(4599):865–7.

19. Piot P, Bartos M, Ghys PD, Walker N, Schwartländer B. The global impact of HIV/AIDS. Nature. 2001 Apr 19;410(6831):968–73.

20. Coffin JM, Hughes SH, Varmus HE. The Place of Retroviruses in Biology. In: Coffin JM, Hughes SH, Varmus HE, editors. Retroviruses. Cold Spring Harbor (NY): Cold Spring Harbor Laboratory Press; 1997.

21. German Advisory Committee Blood (Arbeitskreis Blut), Subgroup 'Assessment of Pathogens Transmissible by Blood'. Human Immunodeficiency Virus (HIV). Transfus Med Hemotherapy. 2016 May;43(3):203–22.

22. Tomás HA, Rodrigues AF, Alves PM, Coroadinha AS. Lentiviral Gene Therapy Vectors: Challenges and Future Directions. In: Martin F, editor. Gene Therapy - Tools and Potential Applications. InTech; 2013.

23. Pluta K, Kacprzak MM. Use of HIV as a gene transfer vector. Acta Biochim Pol. 2009;56(4):531–95.

24. Frankel AD, Young JAT. HIV-1: Fifteen Proteins and an RNA. Annu Rev Biochem. 1998 Jun 28;67(1):1–25.

25. Lentivirus - Introduction | ABM Inc. [Internet]. [cited 2019 Sep 23]. Available from: https://www.abmgood.com/marketing/knowledge_base/The_Lentivirus_System.php

26. Nkeze J, Li L, Benko Z, Li G, Zhao RY. Molecular characterization of HIV-1 genome in fission yeast Schizosaccharomyces pombe. Cell Biosci. 2015 Dec 25;5(1):47.

27. Pollard VW, Malim MH. THE HIV-1 REV PROTEIN. Annu Rev Microbiol. 1998 Oct;52(1):491–532. Available from: http://www.ncbi.nlm.nih.gov/pubmed/9891806

28. Jones KA, Peterlin MB. Control of RNA Initiation and Elongation at the HIV-1 Promoter. Annu Rev Biochem. 1994 Jun 28;63(1):717–43.

29. Rodrigues A, Alves PM, Coroadinha A. Production of Retroviral and Lentiviral Gene Therapy Vectors: Challenges in the Manufacturing of Lipid Enveloped Virus. In: Xu K, editor. Viral Gene Therapy. InTech; 2011.

30. Thomas CE, Ehrhardt A, Kay MA. Progress and problems with the use of viral vectors for gene therapy. Nat Rev Genet. 2003 May;4(5):346–58.

31. Pauwels K, Gijsbers R, Toelen J, Schambach A, Willard-Gallo K, Verheust C, Debyser Z, Herman P. State-of-the-Art Lentiviral Vectors for Research Use: Risk Assessment and Biosafety Recommendations. Curr Gene Ther. 2009 Dec 1;9(6):459–74.

32. Ailles LE, Naldini L. HIV-1-Derived Lentiviral Vectors. In: Current topics in microbiology and immunology. 2002. p. 31–52.

33. Dull T, Zufferey R, Kelly M, Mandel RJ, Nguyen M, Trono D, Naldini L. A third-generation lentivirus vector with a conditional packaging system. J Virol. 1998;72(11):8463–71.

34. Merten O-W, Hebben M, Bovolenta C. Production of lentiviral vectors. Mol Ther Methods Clin Dev. 2016;3:16017.

35. Schweizer M, Merten O-W. Large-Scale Production Means for the Manufacturing of Lentiviral Vectors. Curr Gene Ther. 2010 Dec 1;10(6):474–86.

36. Zufferey R, Dull T, Mandel RJ, Bukovsky A, Quiroz D, Naldini L, Trono D. Self-inactivating lentivirus vector for safe and efficient in vivo gene delivery. J Virol. 1998 Dec;72(12):9873–80.

37. Bokhoven M, Stephen SL, Knight S, Gevers EF, Robinson IC, Takeuchi Y, Collins MK. Insertional gene activation by lentiviral and gammaretroviral vectors. J Virol. 2009 Jan;83(1):283–94.

38. Bray M, Prasad S, Dubay JW, Hunter E, Jeang KT, Rekosh D, Hammarskjöld ML. A small element from the Mason-Pfizer monkey virus genome makes human immunodeficiency virus type 1 expression and replication Rev-independent. Proc Natl Acad Sci U S A. 1994 Feb 15;91(4):1256–60.

39. Roberts TM, Boris-Lawrie K. The 5’ RNA Terminus of Spleen Necrosis Virus Stimulates Translation of Nonviral mRNA. J Virol. 2000 Sep 1;74(17):8111–8.

40. Pandya S, Boris-Lawrie K, Leung NJ, Akkina R, Planelles V. Development of an Rev-Independent, Minimal Simian Immunodeficiency Virus-Derived Vector System. Hum Gene Ther. 2001 May

6;12(7):847–57.

41. Kotsopoulou E, Kim VN, Kingsman AJ, Kingsman SM, Mitrophanous KA. A Rev-independent human immunodeficiency virus type 1 (HIV-1)-based vector that exploits a codon-optimized HIV-1 gag-pol gene. J Virol. 2000 May;74(10):4839–52.

42. McCarron A, Donnelley M, McIntyre C, Parsons D. Challenges of up-scaling lentivirus production and processing. J Biotechnol. 2016 Dec 20;240:23–30.

43. Ansorge S, Henry O, Kamen A. Recent progress in lentiviral vector mass production. Biochem Eng J. 2010 Feb 15;48(3):362–77.

44. Park J, Inwood S, Kruthiventi S, Jenkins J, Shiloach J, Betenbaugh M. Progressing from transient to stable packaging cell lines for continuous production of lentiviral and gammaretroviral vectors. Curr Opin Chem Eng. 2018 Dec;22:128–37.

45. Tomás HA, Rodrigues AF, Carrondo MJT, Coroadinha AS. LentiPro26: Novel stable cell lines for constitutive lentiviral vector production. Sci Rep. 2018;8(1):1–11.

46. Konvalinka J, Litterst MA, Welker R, Kottler H, Rippmann F, Heuser AM, Kräusslich HG. An active-site mutation in the human immunodeficiency virus type 1 proteinase (PR) causes reduced PR activity and loss of PR-mediated cytotoxicity without apparent effect on virus maturation and infectivity. J Virol. 1995 Nov;69(11):7180–6.

47. Page KA, Landau NR, Littman DR. Construction and use of a human immunodeficiency virus vector for analysis of virus infectivity. J Virol. 1990 Nov;64(11):5270–6.

48. Cronin J, Zhang X-Y, Reiser J. Altering the tropism of lentiviral vectors through pseudotyping. Curr Gene Ther. 2005 Aug;5(4):387–98.

49. Joglekar A V., Sandoval S. Pseudotyped Lentiviral Vectors: One Vector, Many Guises. Hum Gene Ther Methods. 2017 Dec 1;28(6):291–301.

50. Mátrai J, Chuah MK, VandenDriessche T. Recent Advances in Lentiviral Vector Development and Applications. Mol Ther. 2010 Mar;18(3):477–90.

51. Lévy C, Verhoeyen E, Cosset F-L. Surface engineering of lentiviral vectors for gene transfer into gene therapy target cells. Curr Opin Pharmacol. 2015 Oct 1;24:79–85.

52. Finkelshtein D, Werman A, Novick D, Barak S, Rubinstein M. LDL receptor and its family members serve as the cellular receptors for vesicular stomatitis virus. Proc Natl Acad Sci U S A. 2013 Apr 30;110(18):7306–11.

53. DePolo NJ, Reed JD, Sheridan PL, Townsend K, Sauter SL, Jolly DJ, Dubensky TW. VSV-G Pseudotyped

Lentiviral Vector Particles Produced in Human Cells Are Inactivated by Human Serum. Mol Ther. 2000 Sep;2(3):218–22.

54. Burns JC, Friedmann T, Driever W, Burrascano M, Yee JK. Vesicular stomatitis virus G glycoprotein pseudotyped retroviral vectors: Concentration to very high titer and efficient gene transfer into mammalian and nonmammalian cells. Proc Natl Acad Sci U S A. 1993 Sep 1;90(17):8033–7.

55. Tomás HA, Mestre DA, Rodrigues AF, Guerreiro MR, Carrondo MJT, Coroadinha AS. Improved GaLV-TR Glycoproteins to Pseudotype Lentiviral Vectors: Impact of Viral Protease Activity in the Production of LV Pseudotypes. Mol Ther - Methods Clin Dev. 2019 Dec 13;15:1–8.

56. Stitz J, Buchholz CJ, Engelstädter M, Uckert W, Bloemer U, Schmitt I, Cichutek K. Lentiviral Vectors Pseudotyped with Envelope Glycoproteins Derived from Gibbon Ape Leukemia Virus and Murine Leukemia Virus 10A1. Virology. 2000 Jul;273(1):16–20.

57. Ikeda Y, Takeuchi Y, Martin F, Cosset F-L, Mitrophanous K, Collins M. Continuous high-titer HIV-1 vector production. Nat Biotechnol. 2003 May 7;21(5):569–72.

58. Sakuma T, De Ravin SS, Tonne JM, Thatava T, Ohmine S, Takeuchi Y, Malech HL, Ikeda Y. Characterization of retroviral and lentiviral vectors pseudotyped with xenotropic murine leukemia virus-related virus envelope glycoprotein. Hum Gene Ther. 2010 Dec;21(12):1665–73.

59. Tözsér J. Comparative Studies on Retroviral Proteases: Substrate Specificity. Viruses. 2010 Jan 14;2(1):147–65.

60. Beck ZQ, Hervio L, Dawson PE, Elder JH, Madison EL. Identification of Efficiently Cleaved Substrates for HIV-1 Protease Using a Phage Display Library and Use in Inhibitor Development. Virology. 2000 Sep;274(2):391–401.

61. Kavanaugh MP, MILLERtI DG, Zhang W, LAWt W, Kozak SL, Kabat D, DUSTY MILLERt A. Cell-surface receptors for gibbon ape leukemia virus and amphotropic murine retrovirus are inducible sodium-dependent phosphate symporters. Proc Nati Acad Sci USA. 1994;91:7071–5.

62. Mestre D. A Novel Generation of Lentiviral Vectors for Gene Therapy. Thesis to obtain a Master's degree in Biotechnology. Universidade Nova de Lisboa; 2016.

63. Christodoulopoulos I, Cannon PM. Sequences in the Cytoplasmic Tail of the Gibbon Ape Leukemia Virus Envelope Protein That Prevent Its Incorporation into Lentivirus Vectors. J Virol. 2001;75(9):4129–38.

64. Cormack BP, Valdivia RH, Falkow S. FACS-optimized mutants of the green fluorescent protein (GFP). Gene. 1996 Jan 1;173(1):33–8.

65. Guerreiro MR, Freitas DF, Alves PM, Coroadinha AS. Detection and Quantification of Label-Free Infectious Adenovirus Using a Switch-On Cell-Based Fluorescent Biosensor. ACS Sensors. 2019 Jun 28;4(6):1654–61.

66. Shaner NC, Campbell RE, Steinbach PA, Giepmans BNG, Palmer AE, Tsien RY. Improved monomeric red, orange and yellow fluorescent proteins derived from Discosoma sp. red fluorescent protein. Nat Biotechnol. 2004;22(12):1567–72.

67. Weiner MP, Costa GL, Schoettlin W, Cline J, Mathur E, Bauer JC. Site-directed mutagenesis of double-stranded DNA by the polymerase chain reaction. Gene. 1994;151(1–2):119–23.

68. Dubridge RB, Tang P, Chao Hsia H, Leong P-M, Miller JH, Calos1 MP. Analysis of Mutation in Human Cells by Using an Epstein-Barr Virus Shuttle System. Mol Cell Biol. 1987;7(1):379–87.

69. Sanjana NE, Shalem O, Zhang F. Improved vectors and genome-wide libraries for CRISPR screening. Nat Methods. 2014 Aug 30;11(8):783–4.

70. Overbaugh J, Miller AD, Eiden M V. Receptors and Entry Cofactors for Retroviruses Include Single and Multiple Transmembrane-Spanning Proteins as well as Newly Described Glycophosphatidylinositol-Anchored and Secreted Proteins. Microbiol Mol Biol Rev. 2001 Sep 1;65(3):371–89.

71. Rodrigues AF, Formas-Oliveira AS, Guerreiro MR, Tomás HA, Alves PM, Coroadinha AS. Single-step cloning-screening method: A new tool for developing and studying high-titer viral vector producer cells. Gene Ther. 2015;22(9):685–95.

72. R Core Team. R: A Language and Environment for Statistical Computing [Internet]. R: A Language and Environment for Statistical Computing. Vienna, Austria; 2014. Available from: https://www.r-project.org/

73. Livak KJ, Schmittgen TD. Analysis of relative gene expression data using real-time quantitative PCR and the 2-ΔΔCT method. Methods. 2001;25(4):402–8.

74. density function | R Documentation [Internet]. [cited 2019 Sep 28]. Available from: https://www.rdocumentation.org/packages/stats/versions/3.6.0/topics/density

75. Kozak M. Effects of intercistronic length on the efficiency of reinitiation by eucaryotic ribosomes. Mol Cell Biol. 1987 Oct;7(10):3438–45.

76. Kozak M. Pushing the limits of the scanning mechanism for initiation of translation. Gene. 2002 Oct 16;299(1–2):1–34.

77. Goswami R, Subramanian G, Silayeva L, Newkirk I, Doctor D, Chawla K, Chattopadhyay S, Chandra D,

Chilukuri N, Betapudi V. Gene Therapy Leaves a Vicious Cycle. Front Oncol. 2019 Apr 24;9:297.

78. Anguela XM, High KA. Entering the Modern Era of Gene Therapy. Annu Rev Med. 2019 Jan 27;70(1):273–88.

79. Montini E, Cesana D, Schmidt M, Sanvito F, Bartholomae CC, Ranzani M, Benedicenti F, Sergi LS, Ambrosi A, Ponzoni M, Doglioni C, Di Serio C, von Kalle C, Naldini L. The genotoxic potential of retroviral vectors is strongly modulated by vector design and integration site selection in a mouse model of HSC gene therapy. J Clin Invest. 2009 Apr;119(4):964–75.

80. Beck L, Leroy C, Salaün C, Margall-Ducos G, Desdouets C, Friedlander G. Identification of a novel function of PiT1 critical for cell proliferation and independent of its phosphate transport activity. J Biol Chem. 2009 Nov 6;284(45):31363–74.

81. Zhang X-H, Tee LY, Wang X-G, Huang Q-S, Yang S-H. Off-target Effects in CRISPR/Cas9-mediated Genome Engineering. Mol Ther - Nucleic Acids. 2015;4:e264.

82. Sundaresan R, Parameshwaran HP, Yogesha SD, Keilbarth MW, Rajan R. RNA-Independent DNA Cleavage Activities of Cas9 and Cas12a. Cell Rep. 2017;21(13):3728.

83. Radhakrishnan P, Basma H, Klinkebiel D, Christman J, Cheng P-W. Cell type-specific activation of the cytomegalovirus promoter by dimethylsulfoxide and 5-aza-2'-deoxycytidine. Int J Biochem Cell Biol. 2008;40(9):1944–55.

84. Wang X, Xu Z, Tian Z, Zhang X, Xu D, Li Q, Zhang J, Wang T. The EF-1α promoter maintains high-level transgene expression from episomal vectors in transfected CHO-K1 cells. J Cell Mol Med. 2017 Nov 1;21(11):3044–54.

Annexes

Plasmids and their main transcriptional units

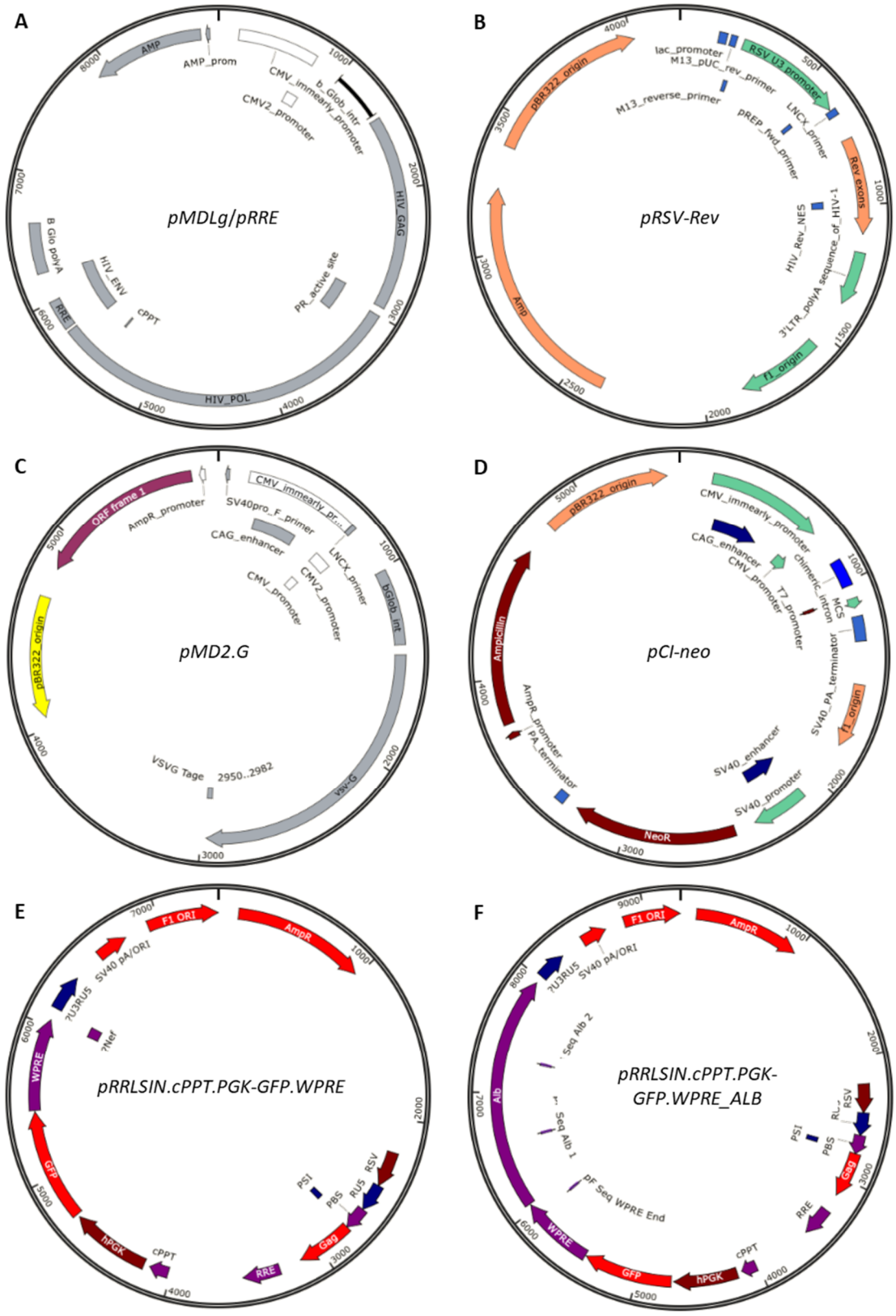

Figure A. 1 – Plasmids used in this work and the respective main transcriptional units. A) Plasmid encoding Gag-Pol polyprotein from HIV-1; B) Plasmid encoding Rev protein; C) Plasmid encoding VSV-G glycoprotein; D) Stuffer plasmid used in the semi-stable production setting (pCI-neo); E) Plasmid encoding eGFP LV transgene; F) Plasmid used to establish the calibration curves for VCN-PCR titration method.

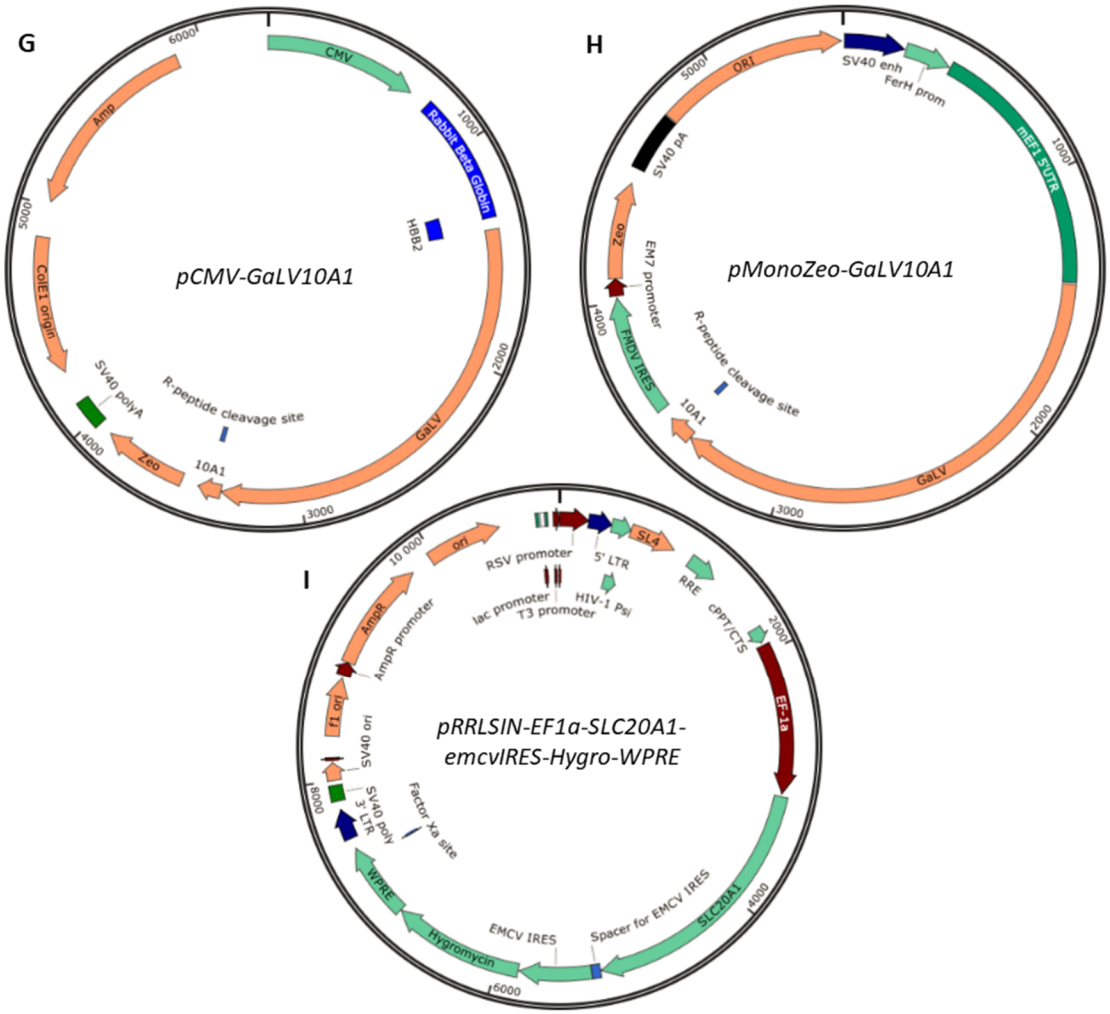

Figure A. 1 - Plasmids used in this work and the respective main transcriptional units (continuation). G) Original plasmid encoding GaLV engineered envelop glycoproteins (here represented *pCMV-GaLV10A1*); H) New plasmids developed for envelope glycoprotein stable expression (here represented *pMonoZeo-GaLV10A1*); I) Plasmids developed for complementation studies (here represented the plasmid encoding SLC20A1 protein).

PCR amplification efficiency for GaLV10A1 enginneered envelope glycoproteins

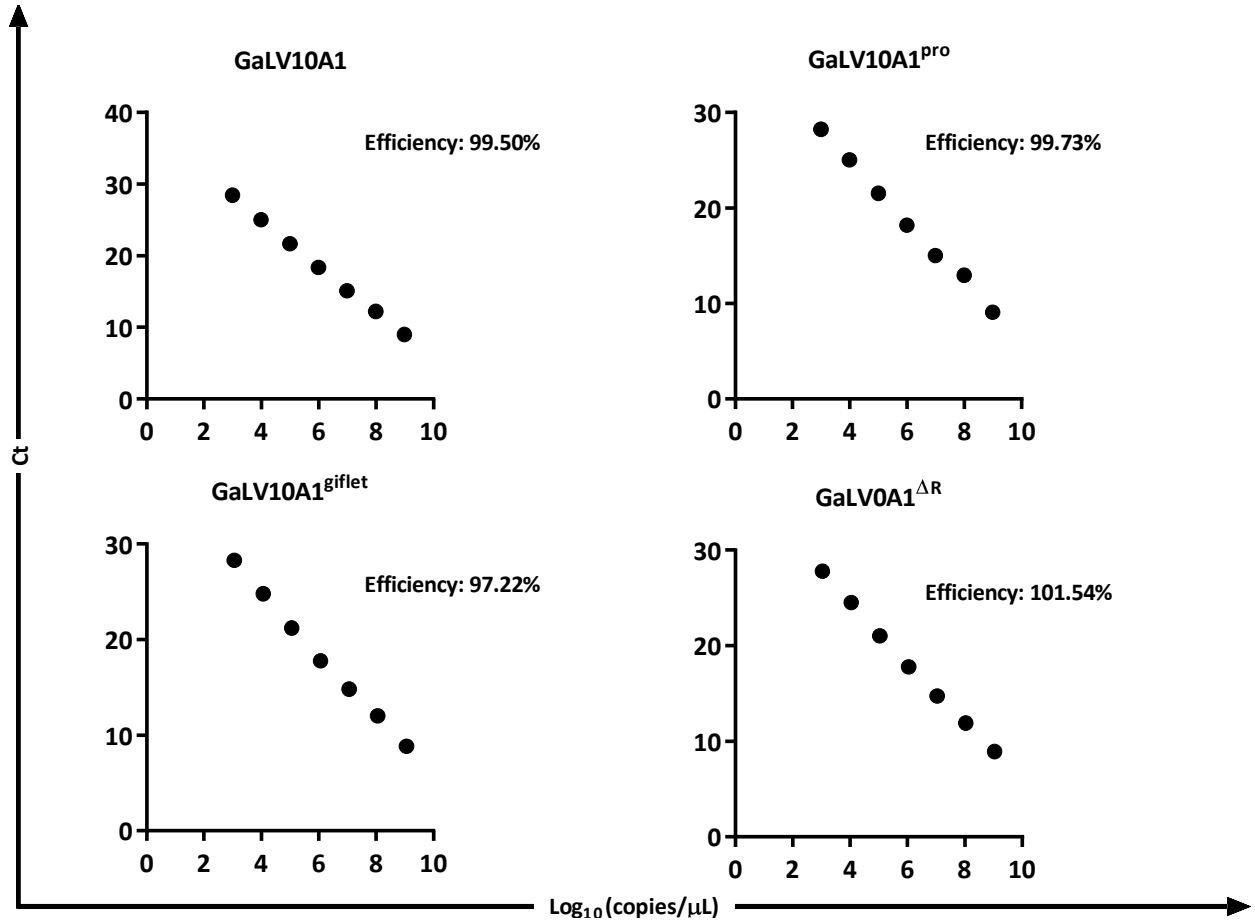

Figure A. 2 - Assessment of PCR amplification efficiency for the different GaLV10A1 envelope glycoprotein plasmids. PCR amplification efficiency for *pMonoZeo-GaLV10A1*, or its derivates, was determined by RT-qPCR through the slope value of calibration curves. These calibration curves were established with ten-fold dilutions of plasmids with known concentration ranging from 1 x 10^8 to 1 x 10^2 copies of plasmid DNA per µL (copies/µL). The first two points from each calibration curves were excluded from the amplification efficiency calculation. Ct: crossing threshold.

Primers and templates used for molecular cloning

Table A. 1 - Primers and templates for plasmid cloning

Construct	Insert			Vector	
	Fragment	Source	Primers	Parental	Primers/restriction enzymes
pMonoZeo-GaLV10A1	*GaLV10A1*	*pCMV-GaLV10A1*	pF-ATTCAAAGCAACCGGTACCATGGTATTGCTGCCTGG	*pMonoZeo-4070A*	AgeI BamHI
pMonoZeo-GaLV10A1pro	*GaLV10A1^{pro}*	*pCMV-GaLV10A1pro*			
pMonoZeo-GaLV10A1giflet	*GaLV10A1^{giflet}*	*pCMV-GaLV10A1giflet*	pR-AGCGGATAACGGATCCTTAATTGTCAACACTAGGCGCCC		
pMonoZeo-GaLV10A1ΔR	*GaLV10A1^{ΔR}*	*pCMV-GaLV10A1ΔR*			
pRRLSIN.cPPT.PGK-GFP.WPRE_ALB	*ALB*	*pDONR221 ID: HsCD00043431*	pF-TGCAATTCGATGAAGTGGGTAACCTTTATTTCCC	*pRRLSIN.cPPT.PGK-GFP.WPRE*	KpnI
			pR-TCATTGGTCTTAAAGTCACTTATCGTCGTCATCCTTG		
pSLC20A1	-	-	-	*pDONR221 ID: HsCD00045579*	pF- Phosf-GCTTCCCAGCGTGGACTTGAAAGAGG
					pR- Phosf-CTCTCTCTCTCTGGAGCTTCCTCCAA
pRRLSIN-EF1a-SLC20A2-emcvIRES-Puro-WPRE	*SLC20A2*	*pDONR221 ID: HsCD00043621*	pF- AGCTTGGTACGCTAGCATGGCCATGGATGAGTATTT	*pRRLSIN-EF1a-CRE-emcvIRES-Puro-WPRE*	NheI BsiWI
			pR- ATTTCGCGGGCGTACGCTACACATATGGAAGGATCC		
pRRLSIN-EF1a-SLC20A2-emcvIRES-Hygro-WPRE	*hygro^{R}*	*pREV-Hygro-WPRE*	pF- CGATGATAATACTAGTACCATGAAGAAACCTGAACTGACAG	*pRRLSIN-EF1a-SLC20A2-emcvIRES-Puro-WPRE*	SpeI SalI
			pR- GAGGTTGATTGTCGACTCATTCCTTGGCTCTGGGTC		
pRRLSIN-EF1a-SLC20A1-emcvIRES-Hygro-WPRE	*SLC20A1*	*pSLC20A1*	pF- AGCTTGGTACGCTAGCATGGCAACGCTGATTACCAG	*pRRLSIN-EF1a-SLC20A2-emcvIRES-Hygro-WPRE*	NheI BsiWI
			pR- ATTTCGCGGGCGTACGCTACATTCTGAGGATGACAT		
pRRLSIN-EF1a-mCherry-emcvIRES-Puro-WPRE	*mcherry*	*pPuro_ mCherry NheI*	pF- AGCTTGGTACGCTAGCCCACCATGGTGAGCAAGGG	*pRRLSIN-EF1a-SLC20A2-emcvIRES-Hygro-WPRE*	NheI BsiWI
			pR- ATTTCGCGGGCGTACGGCTAGCTTACTTGTACAGCTCGTCC		

Library of sgRNA used in the establishment of HEK 293T SLC20A1 KO

Table A. 2 - Library of sgRNA used in SLC20A1 knock-out strategy by CRISPR/Cas9.

sgRNA	Sequence
V1 sgRNA	ATAGCTATTATTGCGCCTTA
V2 sgRNA	TAGCTATTATTGCGCCTTAA
V3 sgRNA	CTCCAAGAAGCGAATTCGAA

Primers and probes used for RT-qPCR

Table A. 3 – Primers and probes used for RT-qPCR.

Gene	Sequence
SLC20A1	pF - GGCAGAGATGGGTCTAGGTG
	pR - TTGGTGTTGCCACTTTTGAA
SLC20A2	pF - CCCCAGAGGACAGTGAGAAG
	pR - GGAAATGGAACAGGAGGTGA
RPL22	pF - CTGCCAATTTTGAGCAGTTT
	pR - CTTTGCTGTTAGCAACTACGC
GaLV	pF - GGACCAAAATAGCGAATGGA
	pR - GGTGAACTGTACGCCTGGAT
LTR	pF - GCTAACTAGGGAACCCAC
	pR - GCTAGAGATTTTCCACACTGA
LTR probe	HEX/CTTGCCTTG/ZEN/AGTGCTTCAAGTAGTG/IBFQ